Carnegie Mellon University

CARNEGIE INSTITUTE OF TECHNOLOGY

THESIS

SUBMITTED IN PARTIAL FULFILLMENT OF THE REQUIREMENTS

FOR THE DEGREE OF Doctor of Philosophy

TITLE Integrating Variable Renewables into the Electric Grid: An Evaluation of Challenges and Potential Solutions

PRESENTED BY Colleen A. Lueken

ACCEPTED BY THE DEPARTMENT OF

Engineering and Public Policy

ADVISOR, MAJOR PROFESSOR DATE

DEPARTMENT HEAD DATE

APPROVED BY THE COLLEGE COUNCIL

DEAN DATE

UNIVERSIDADE TÉCNICA DE LISBOA
INSTITUTO SUPERIOR TÉCNICO

Integrating Variable Renewables into the Electric Grid: An Evaluation of Challenges and Potential Solutions

Colleen Angela Lueken

Co-supervisors: Doctor Jay Apt (Co-Chair)
Doctor Pedro M.S. Carvalho (Co-Chair)

Thesis approved in public session to obtain the PhD Degree in
Engineering and Public Policy

Jury Final Classification:

Jury

Chairs: Doctor Jay Apt
Doctor Pedro M.S. Carvalho

Members of the Committee:
Doctor Luis Marcelino Ferreira
Doctor Gabriela Hug
Doctor Granger Morgan

2012

Integrating Variable Renewables into the Electric Grid: An Evaluation of Challenges and Potential Solutions

Submitted in partial fulfillment of the requirements for

the degree of

Doctor of Philosophy

in

Engineering and Public Policy

Colleen A. Lueken

B.S., Aerospace Engineering, Massachusetts Institute of Technology
M.E.P.P., Engineering and Public Policy, University of Maryland

Carnegie Mellon University
Pittsburgh, PA

December 2012

Copyright 2012 © by Colleen Angela Lueken. All rights reserved.

Abstract

Renewable energy poses a challenge to electricity grid operators due to its variability and intermittency. In this thesis I quantify the cost of variability of different renewable energy technologies and then explore the use of reconfigurable distribution grids and pumped hydro electricity storage to integrate renewable energy into the electricity grid.

Cost of Variability

I calculate the cost of variability of solar thermal, solar photovoltaic, and wind by summing the costs of ancillary services and the energy required to compensate for variability and intermittency. I also calculate the cost of variability per unit of displaced CO_2 emissions. The costs of variability are dependent on technology type. Variability cost for solar PV is $8-11/MWh, for solar thermal it is $5/MWh, and for wind it is around $4/MWh. Variability adds ~$15/tonne CO_2 to the cost of abatement for solar thermal power, $25 for wind, and $33-$40 for PV.

Distribution Grid Reconfiguration

A reconfigurable network can change its topology by opening and closing switches on power lines. I show that reconfiguration allows a grid operator to reduce operational losses as well as accept more intermittent renewable generation than a static configuration can. Net present value analysis of automated switch technology shows that the return on investment is negative for this test network when considering loss reduction, but that the return is positive under certain conditions when reconfiguration is used to minimize curtailment of a renewable energy resource.

Pumped Hydro Storage in Portugal

Portugal is planning to build five new pumped hydro storage facilities to balance its growing wind capacity. I calculate the arbitrage potential of the storage capacity from the perspective of an independent storage owner, a thermal fleet owner, and a consumer-oriented storage owner. This research quantifies the effect storage ownership has on CO_2

emissions, consumer electricity expenditure, and thermal generator profits. I find that in the Portuguese electricity market, an independent storage owner could not recoup its investment in storage using arbitrage only, but a thermal fleet owner or consumer-oriented owner may get a positive return on investment.

Acknowledgements

I have been supported throughout my PhD research by a grant from the Portuguese Foundation for Science and Technology (Fundação para a Ciência ea Tecnologia). The CMU-Portugal program has been a unique and rewarding experience and I am grateful to have had the support and resources from both Carnegie Mellon University and Instituto Superior Técnico behind my PhD research.

In addition this work was supported in part by grants from the Alfred P. Sloan Foundation and the Electric Power Research Institute to the Carnegie Mellon Electricity Industry Center; from the Doris Duke Charitable Foundation, the RK Mellon Foundation, and the Heinz Endowments to the RenewElec program at Carnegie Mellon University.

For their advice and helpful conversations over the course of my research I would like to thank Roger Dugan, Luis Marcelino Ferreira, Emily Fertig, Mark Karl, Warren Katzenstein, Lester Lave, Bart McManus, Jared Moore, Terry Oliver, Gregory Reed, James Stoupis, and Le Tang. I have benefitted greatly from those willing to share data with me for research purposes: Tom Hansen for solar PV generation data and others wishing to remain anonymous. I am grateful to ERCOT, CAISO, MIBEL, and PJM for making significant amounts of data publically available.

I would also like to thank Patti Steranchak, Patty Porter, Victoria Finney, Barbara Bugosh, Adam Loucks, Ana Mateus, Nicole Hillard and the rest of the EPP and CMU-Portugal staff for all of their help and support.

I am grateful for the support and guidance of my advisors Jay Apt and Pedro Carvalho, and the rest of my thesis committee: Luis Marcelino Ferreira, Gabriela Hug, and Granger Morgan.

Finally I would like to thank my friends and family, especially my husband, Roger Lueken, and my parents, Dru and Bill Horin.

Table of Contents

List of Figures

List of Tables

1. Introduction

Policies aimed at increasing the amount of electricity generated from renewable energy have forced electric utilities to rethink how to reliably deliver power to their customers at reasonable costs. Compounding the problem, the electricity industry is traditionally conservative and slow to adopt new technologies. However, inaction is not an option when utilities must increasingly rely on variable power output from renewables to meet demand. In this thesis I present an explanation of why the variability of renewable energy poses a challenge to the electricity industry. Then, I explore two strategies for better integrating renewables into the electric grid: flexible distribution grids and pumped hydro electricity storage.

As a joint PhD student at Carnegie Mellon University in Pittsburgh and Instituto Superior Técnico in Lisbon, I have researched these issues from both American and European perspectives. The European Union (EU) has enacted the 20-20-20 initiative, which encourages growth in the renewable energy industry. Specifically, the initiative calls for 20% of all energy consumption in the EU to come from renewable sources by 2020. In addition to the EU policy, Portugal mandates that 30% of their energy consumption and 60% of electricity generation come from renewable sources by 2020.

While there is no national equivalent in the United States to the EU policies encouraging renewable energy consumption, many states have enacted renewables portfolio standards (RPSs) to encourage the development of renewable energy. California, for example, mandates that 33% of its electricity come from renewable sources by 2020. In addition to the RPS, many states have favorable policy environments for building distributed renewable generation, including rooftop solar PV panels, that can change the demand profile of loads. Large utilities in states with RPSs must decide how to invest in a portfolio of renewable energy technologies to fulfill their requirements. Utilities also must decide how to invest in distribution grid upgrades in light of a changing system with more distributed renewable generation, the possibility of demand response, and perhaps electric vehicles.

In Chapter 2, I explain why variable power outputs from renewable generators increase costs for an electric utility by comparing the costs of power output variability of wind, solar photovoltaic, and concentrated solar power (CSP) technologies. This is an important issue because some state governments have enacted set-aside requirements for solar photovoltaic (PV) power or other technologies within an RPS. The purpose of these set-asides is to bolster a certain generator type in the state. However, because the costs of interconnecting different renewable resources to the electricity grid vary based on the resource's variability characteristics, such set-asides can increase the cost of providing electricity. I find that solar PV creates the highest variability costs, and CSP and wind create lower variability costs for a grid operator.

In Chapter 3, I present an analysis of one option to help integrate renewable energy into distribution grids. Reconfigurable electric grids have switches on their lines, which allows an operator to change the configuration of the grid in order to better accommodate renewable energy power output or reduce losses on the lines. A reconfigurable network can change its topology by opening and closing switches on power lines. Using real wind, solar, load, and cost data and a model of a reconfigurable distribution grid, I show that reconfiguration allows a grid operator to reduce operational losses as well as accept more intermittent renewable generation than a static configuration can. Net present value analysis of automated switch technology shows that the return on investment is negative for this test network when considering only loss reduction, but that the investment is attractive under certain conditions when reconfiguration is used to minimize curtailment.

Chapter 4 contains an analysis of Portugal's investment in pumped hydro electricity storage from an energy arbitrage standpoint. Portugal plans to increase its pumped hydro storage capacity 60% by 2020 to accommodate an increasing penetration of variable renewable electricity. Such an increase in storage capacity and renewables has the potential to affect the market price of electricity in the Iberian market, MIBEL. I use a nonlinear optimization program to analyze the affect of storage on market prices, consumer expenditures, thermal generator profits, and storage owner profits. I also explore the effect of ownership structure on storage operation. Independent storage owners, those who own thermal generation assets, and consumer-owners all operate storage differently according to their profit-maximizing objective functions.

2. The Costs of Solar and Wind Power Variability for Reducing CO_2 Emissions[a]

2.1 Introduction

The variability and intermittency of wind and solar electricity generators add to the cost of energy by creating greater demand for balancing energy and other ancillary services. As these sources begin to provide a larger fraction of the electricity supply, the relative costs of their variability and the cost of variability for CO_2 emissions reduction may become important considerations in selection of technologies to meet renewables portfolio standards (RPSs).

I quantify the differences in variability among three types of renewable electricity generation: solar thermal, solar photovoltaic (PV), and wind, using power spectrum analysis. The power spectrum analysis in this paper follows the method used by Apt.[1] Katzenstein et al. have examined wind variability using power spectra, and have shown that variability of a single wind farm can be reduced by 87% by interconnecting four wind farms, but additional interconnections have diminishing returns.[2] In addition, I demonstrate how these differences in power spectra translate into different costs of variability.

Katzenstein and Apt calculate the cost of wind power variability, and my analysis of the cost of variability of all three technologies uses a similar method.[3] I focus on sub-hourly variability to calculate the cost of variability to a scheduling entity. Solar variability at sub-hourly time scales is caused by the movement of clouds across the sky; wind variability on this time scale is caused by turbulence and weather patterns.

Lavania et al. examined solar variability in the frequency domain, and propose a method to reduce variability by interconnecting solar plants, but they use solar insolation data to estimate power output rather than actual solar array power output data.[4] Gowrisankaran et al. present an economic model to calculate the cost of solar power intermittency in a

[a] Significant portions of this chapter appear in: Colleen Lueken, Gilbert Cohen, Jay Apt. 2012. *The Cost of Solar and Wind Power Variability for Reducing CO_2 Emissions*. Environmental Science & Technology: Vol. 46 (17), pp. 9761–9767.

grid with high levels of solar penetration.[5] They scale the power output of a 1.5 kW test solar facility in Tucson to simulate the solar power output. Researchers at LBNL compare the variability and variability costs of solar PV and wind using solar insolation and wind speed data.[6]

Reducing CO_2 emissions is a motivating factor behind integrating renewables into the electricity grid. Dobesova et al. calculated the cost of reducing CO_2 emissions through the Texas RPS, taking into account the added costs of transmission, wind curtailments, production tax credits, and RPS administration.[7] My calculation adds to their work by including only the cost of obtaining balancing and ancillary services for sub-hourly variability of the renewable resource per tonne of CO_2 abatement.

This research differs from earlier solar PV studies because I use real power output data from operational utility-scale plants to calculate the variability and cost of variability. To my knowledge this is the first work to examine the variability and cost of variability of solar thermal power using real power output data. I also show how variability affects CO_2 emissions abatement. Comparing the costs of the three technologies can inform policy discussions about requiring technology set-asides for RPSs.

I find that at frequencies greater than $\sim 10^{-3}$ Hz (corresponding to times shorter than ~ 15 minutes) solar thermal generation is less variable than generation from wind and considerably less variable than solar PV. Using energy and ancillary service prices from California, the cost of variability of a solar thermal facility would be \$5 per MWh. This compares to a cost of variability at a solar PV facility of \$8-11 per MWh. In contrast to solar PV arrays, solar thermal facilities can ride through short periods of reduced insolation due to the thermal inertia of the heat stored in the working fluid, so I would expect a higher cost of variability in solar PV compared to solar thermal. Using the same 2010 California energy and ancillary service prices, the average cost of variability at 20 Electric Reliability Council of Texas (ERCOT) wind farms was \$4 per MWh. Variability adds ~\$15/tonne CO_2 to the cost of abatement for solar thermal power, \$25 for wind, and \$33-\$40 for PV.

2.2 Methods and Data

2.2.1 Data

I obtained 1-minute energy data gathered over a full year from a 4.5 MW solar photovoltaic (PV) array near Springerville, Arizona (in 2005), and 5-minute energy data from Nevada Solar One (NSO), a 75 MW solar thermal generation facility near Boulder City, Nevada (in 2010). I also use 1-minute energy data from a 20 MW+ class solar PV array (provided on the condition of anonymity). I use 15-minute wind data from 20 ERCOT wind farms from 2008.

I use data from the California Independent Service Operator (CAISO) for up and down regulation (in the day-ahead, DAH, market) and energy prices. The 2010 CAISO energy prices represent the Southern California Edison (SCE) utility area real time hourly averages. I use the same price data for all simulations to eliminate the effects of price variations in different years and in different geographic regions. The SCE data (Table 2-1) were chosen to represent a geographical area close to the solar generation facilities in the Southwest. Figure 2-1 is a time series representation of the Springerville solar PV and NSO solar thermal data sets.

Table 2-1. Average price information for CAISO price data used in analysis

Type of charge	Average hourly price per MWh
CAISO SCE Energy (2010)	$42
CAISO SP-15 Energy (2005)	$56
CAISO DAH Up Regulation (2010)	$5.6
CAISO DAH Down Regulation (2010)	$5.0

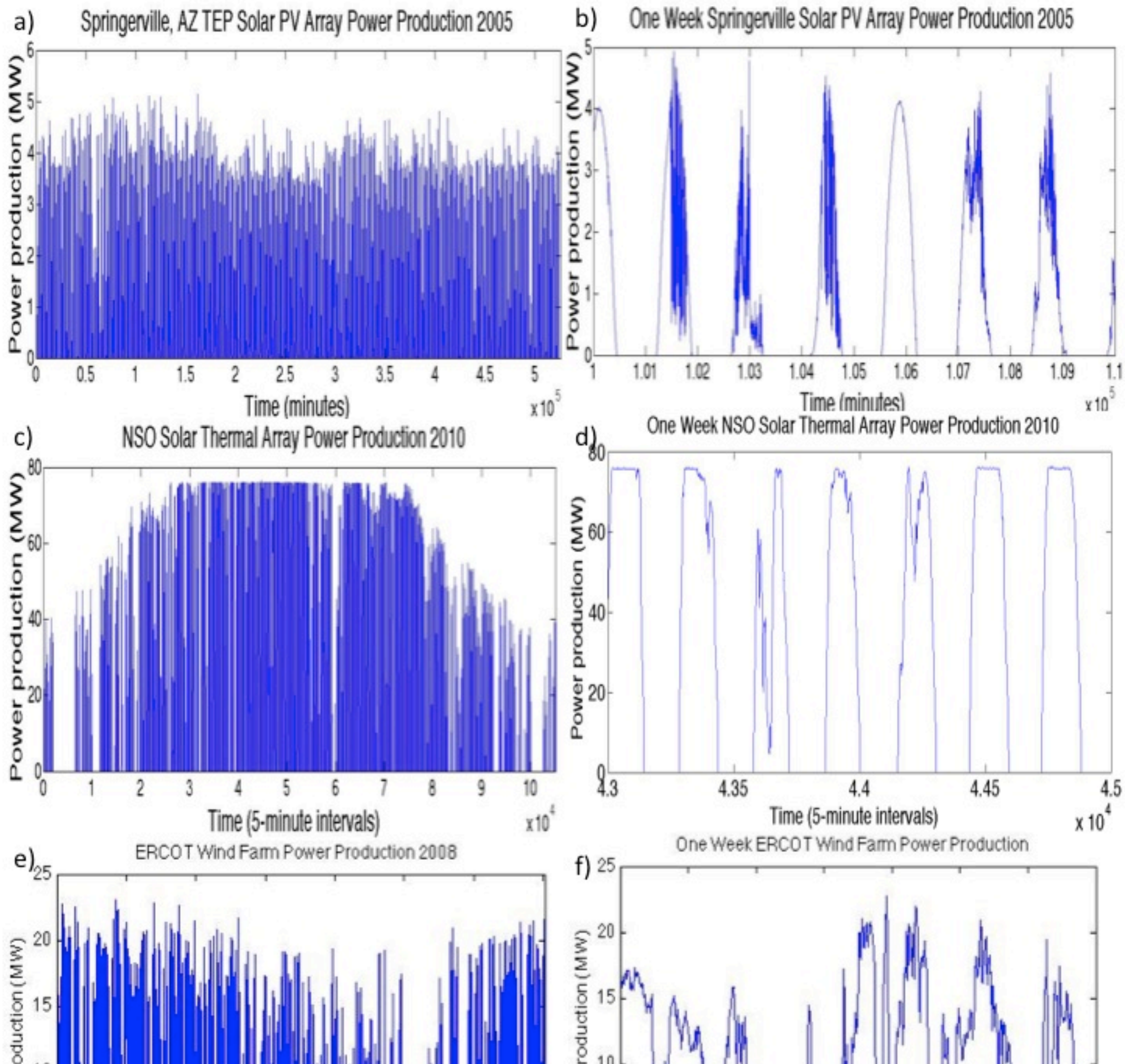

Figure 2-1. Solar thermal and solar PV data: (a) 2005 Springerville PV data; (b) One week of 2005 Springerville PV data; (c) 2010 NSO solar thermal data (the data gaps near the beginning and end of the year represent times the plant was out of service); (d) One week of NSO solar thermal data; (e) 2008 single ERCOT wind farm data; (f) One week of 2008 single ERCOT wind farm data

I obtained data from EPA's Clean Air Markets Data and Maps website on hourly emissions and electricity production for each thermal generating unit greater than 25 MW capacity in California for 2010.[8] Using these data I calculate the cost of variability per unit of displaced CO_2 emissions.

2.2.2 Power Spectral Analysis

As described in Apt,[1] I examine the frequency domain behavior of the time series of power output data from the generation plants by estimating the power spectrum (the power spectral density, PSD). I compute the discrete Fourier transform of the time series. The highest frequency that can be examined in this manner, f_{max}, is given by the Nyquist sampling theorem as half the sampling frequency of the data (i.e. 8.3×10^{-3} Hz for 1–minute data). One of the attributes of power spectrum estimation through periodograms is that increasing the number of time samples does not decrease the standard deviation of the periodogram at any given frequency f_k. In order to take advantage of a large number of data points in a data set to reduce the variance at f_k, the data set may be partitioned into several time segments. The Fourier transform of each segment is then taken and a periodogram estimate constructed. The periodograms are then averaged at each frequency, reducing the variance of the final estimate by the number of segments (and reducing the standard deviation by the reciprocal of the square root of the number of segments). Here I use 16 segments. This has no effect on f_{max}, but increases the lowest non-zero frequency by a factor equal to the number of segments (i.e. for data sampled for a year, the lowest frequency is increased from 3.2×10^{-8} to 5.1×10^{-7} Hz for 16 segment averaging).

The PSD gives a quantitative measure of the ratio of fluctuations at high frequency to those at low. It is fortunate that the PSD of wind, PV, and solar thermal are not flat (white noise). If that were true, large amounts of very fast-ramping sources would be required to buffer the fluctuations of wind and solar power. The observed spectra show that the power fluctuations at frequencies corresponding to 10 minutes, for example, is at least a factor of a thousand smaller than those at periods of 12 hours. Thus, slow-ramping generators (e.g. coal or combined-cycle gas) can compensate for the majority of variability.

2.2.3 Cost of Variability

I calculate the cost of mitigating variability in the generation output by adding the costs of ancillary services and the energy costs required for the ISO to handle intra-hourly variability of the solar or wind resource.[3] The ancillary service cost includes the cost of providing up and down regulation for each hour of operation. The energy term is the absolute value of deviation from the hourly prediction to reflect the cost to the ISO when the generator deviates from its expected production. I use the absolute value of deviation because any deviation from the expected production obligates the ISO to pay a premium to traditional generators to either ramp down, to accommodate the must-take energy from the variable generator, or ramp up to make up for underproduction. I average cost of variability in each hour of the year and normalize the average by the total annual energy produced by the generator. Figure 2 is a graphical representation of the calculation; the ISO uses load following energy and up and down regulation to mitigate the effects of variability of the renewable generation. An ISO would also use frequency response ancillary services to mitigate the very short-term (1-10 second) effects of variability, but that is outside the scope of this research because my datasets contain generation information down to only 1-, 5- or 15-minute granularity. Calculation of the cost of variability is per Equation 2-1 and Equation 2-2.

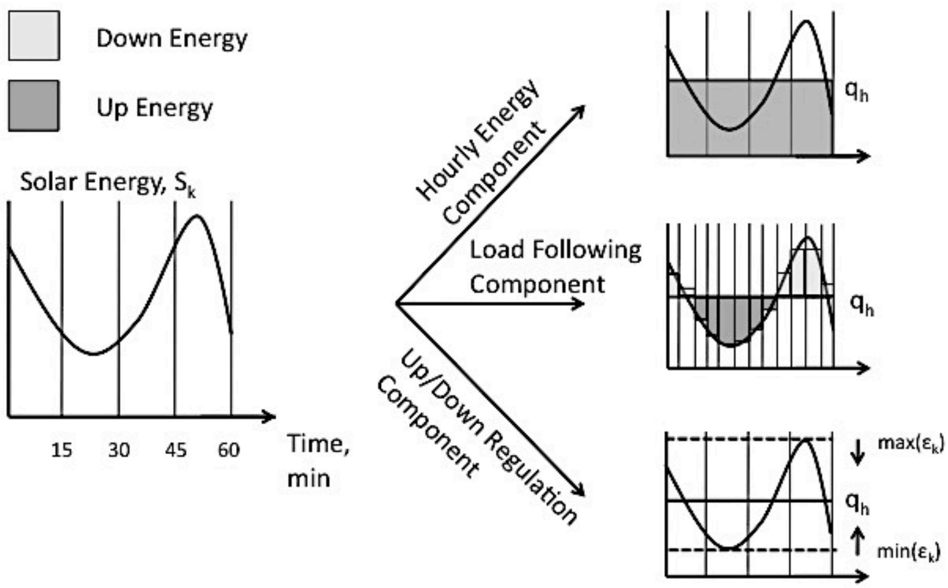

Figure 2-2. Utilities use load following and regulation services to compensate for variability in solar and wind energy. When the energy production, S_k, deviates from the hourly energy set point, q_h, the ISO uses load following regulation to ramp down or supplement the system-wide generation (middle-right graph). In addition, the ISO utilizes up and down regulation equivalent to the minimum and maximum deviation from q_h, respectively (lower right graph).

Equation 2-1
$$\text{Variability Cost}(h) = \sum_{k=1:n} |\varepsilon_k| P_h / n + P_{up,h} \min(\varepsilon_k) + P_{dn,h} \max(\varepsilon_k)$$

Equation 2-2
$$\text{Annual Average Variability Cost} = \frac{\sum_{\boldsymbol{h=1:8760}} \text{Variability Cost}(h)}{\sum_{\boldsymbol{h=1:8760}} \sum_{\boldsymbol{k=1:n}} \boldsymbol{S_{k,h}/n}}$$

Table 2-2. Description of variables associated with Equations 2-1 and 2-2.

Variable	Description
P_h	the hourly price of energy
$P_{up,h}$	the hourly price of up regulation
$P_{dn,h}$	the hourly price of down regulation
q_h	the amount of firm hourly energy scheduled in hour h (calculated as the mean of all $S_{k,h}$ in hour h
$S_{k,h}$	the actual subhourly production of energy in hour h
$\varepsilon_k = S_{k,h} - q_h$	the difference between energy scheduled and produced in segment k of hour h
n	is the number of energy production records per hour (60 for Springerville PV, 12 for NSO, 4 for ERCOT wind, and 60 for the 20 MW+ PV array)

The scheduled hourly energy production, q_h, is the mean of all $S_{k,h}$ for hour h. In reality, an ISO would schedule q_h according to forecast data. By using actual energy production data instead, I calculate a lower bound estimate of actual variability costs. The second two terms in Equation 2-1 represent the cost of up and down regulation for the hour. Even if variable power output averages to the scheduled q_h over an hour, the variable generator creates intra-hourly variability costs for the ISO. Sub-hourly energy scheduling intervals would reduce the costs of variability from wind and solar.

Simulating the cost of variability using energy forecast data would give more information about the realistic costs of intermittency of wind, solar thermal and PV. Actual forecast data for the RE generators in my analysis are unavailable, so I simulated solar forecast data using National Renewable Energy Laboratory's System Advisor Model (SAM) in order to more closely simulate utility operations. I include the analysis of SAM forecast data in Appendix 2A.

Katzenstein and Apt's method is similar, but instead of using the average hourly power production to set q_h, they create an objective function to minimize the intermittency cost with the q_h as the decision variable.[3] Comparing their method to ours, I find similar results and have chosen to use the average energy method to reduce computation times.

It would be possible instead to calculate the variability cost of net load (load minus output from one RE generator). However, the cost of net load variability is highly dependent on the magnitude of the load relative to the capacity of the variable generator under consideration. The variability signals of small generators, such as the 4.5 MW Springerville PV array, are dominated by the variability signals of much larger load regions, such as CAISO. This calculation is meant to indicate of variability cost of an RE generator independently of its size and of the magnitude and variability of demand in its region.

I assume that all plants considered are price takers, not large enough to influence the market price for electricity. I also assume that the balancing energy price is equivalent to the market average hourly energy price.

2.2.4 Cost of Variability and Emissions Displacement

One goal of utilizing renewable energy for electricity is reducing carbon dioxide emissions. I first calculate the cost of solar and wind variability on a per megawatt-hour basis. I also calculate the cost of solar and wind variability per unit of avoided emissions.

I define avoided emissions, $E_{avoided}$, as the difference between the emissions displaced by using renewable energy, $E_{displaced}$, and the emissions created, $E_{ancillary}$, from ancillary services that support the renewable power provider. $E_{displaced}$ represents the avoided emissions due to displacing marginal generating units with must-take renewable electricity generation. $E_{ancillary}$ represents the additional emissions created because of reserve, balancing, and frequency support for the solar or wind resource.

Equation 2-3

$$E_{avoided} = E_{displaced} - E_{ancillary}$$

In any given hour, the cost of avoided emissions is equivalent to the cost of variability divided by the mass of avoided emissions.

Equation 2-4

$$Cost_{avoided\_emissions} = Variability\ Cost/E_{avoided}$$

CAISO also pays for spinning reserve, generating units that are running and emitting CO_2 but not providing power to the grid, to balance variable resources. However, calculating the emissions due to ancillary services is outside the scope of this research, so I disregard the term $E_{ancillary}$ in my calculation. This calculation is meant to be a lower-bound estimate of variability cost per emissions avoided, but one that treats solar thermal, PV, and wind in the same way.

I calculate $E_{displaced}$ for each hour of the year based on the emissions of the marginal generating units and the quantity of power being supplied by the RE generating facility. For each hour, I assume that the most recently switched on unit or units will be displaced by power from a solar or wind generator. If more than one unit is dispatched in the same hour, I calculate the average emissions factor of these units. I do not construct a dispatch model, but rather use the observed hourly plant dispatch for California in 2010 per EPA's Clean Air Markets data.[8] If the solar or wind power generation for that hour surpasses the power production of the marginal unit(s), I identify the next most recently turned on unit until the sum of marginal power surpasses the solar power generated. Figure 2-3 illustrates how the 1^{st}, 2^{nd}, etc. marginal units are defined.

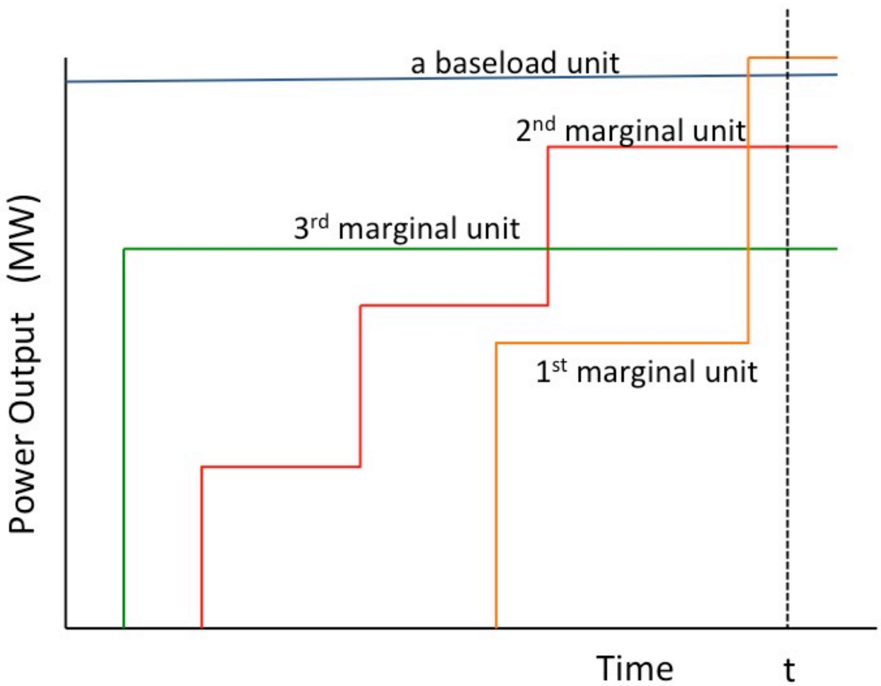

Figure 2-3. Power output of individual generating units over time. The notation of "1^{st} marginal unit" indicates the last unit to be dispatched; the 2^{nd} marginal unit is the next-to-last, and so forth.

The marginal emissions factor in any given hour is

Equation 2-5

$$MEF(h) = \sum_{i=1}^{U} MU_{emissions}(i,h) \,/ \sum_{i=1}^{U} MU_{power}(i,h)$$

Table 2-3. Description of variables used in Equation 2-5

Variable	Description
MEF(h)	is the marginal emissions factor in hour *h*
i	a marginal power plant unit operating in hour *h*
U	is the number of relevant marginal units operating in hour *h*
$MU_{emissions}(i,h)$	is the CO_2 emissions rate of marginal unit *i* in hour *h*
$MU_{power}(i,h)$	is the power output of marginal unit *i* in hour *h*

2.3 Results

2.3.1 Power Spectral Analysis

I follow the method of Apt to calculate the power spectra of a solar thermal plant, a solar PV array, and a wind plant.[1] Graphing multiple power sources together and normalizing the spectra at a frequency corresponding to a range near 24 hours reveals a difference in the variability of each source at high frequencies (Figure 2-4).

The power spectral analysis shows that solar photovoltaic electricity generation has approximately one hundred times larger amplitude of variations at frequencies near 10^{-3} Hz than solar thermal electricity generation (this frequency corresponds to ~ 15 minutes). Electricity from wind farms is intermediate between solar PV and solar thermal in terms of variability in this frequency range. High variability at frequencies corresponding to less than one hour creates the need for more ancillary energy services to avoid quality problems or interruptions in electricity service to customers.

Both types of solar generation exhibit strong peaks corresponding to a 24-hour period and its higher harmonics, as expected from the cessation of generation each night. Wind power exhibits this property to a lesser extent (in the continental US, wind tends to have a diurnal variation, blowing more strongly at night).

The power spectra are similar for the three generation types at frequencies lower than $\sim 4 \times 10^{-5}$ Hz (corresponding to periods greater than six hours).

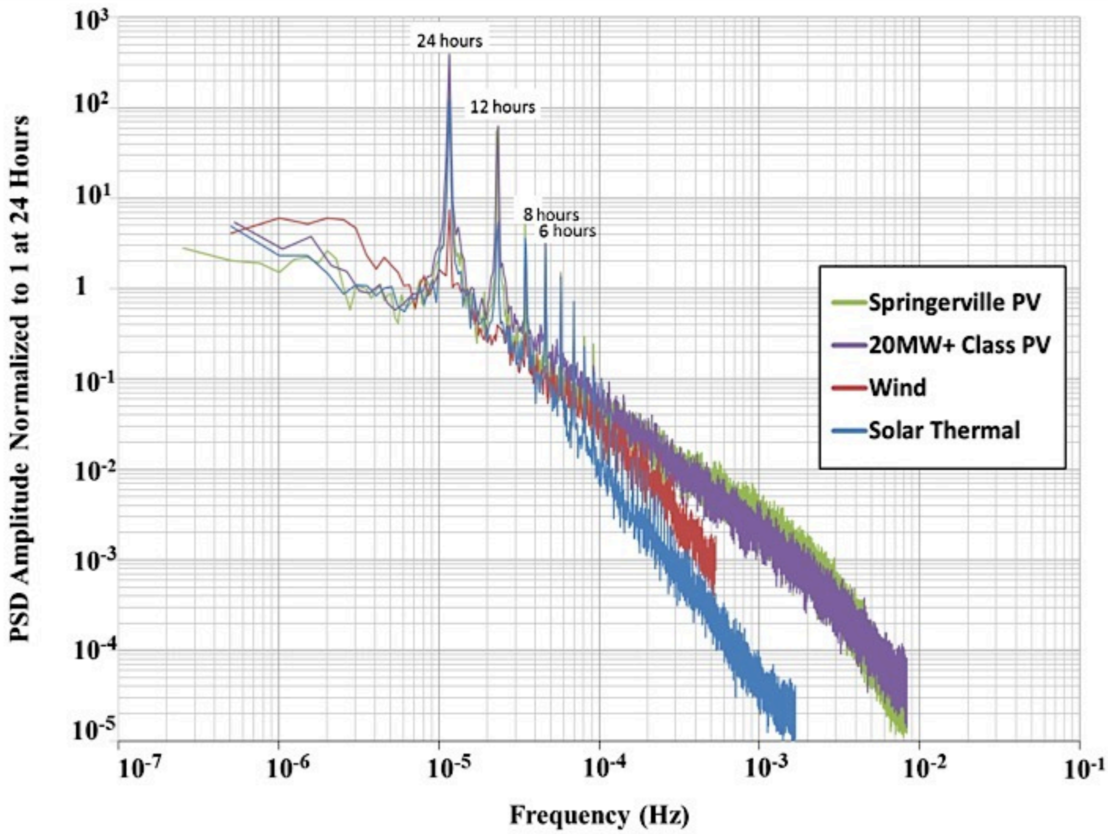

Figure 2-4. Power spectra of solar PV, wind, and solar thermal generation facilities. The spectra have been normalized to one at a frequency corresponding to approximately 24 hours. All spectra are computed using 16-segment averaging. The strong diurnal peaks of solar power, and weaker one for wind power (along with their higher harmonics) are evident. There is very little difference between the 5 MW Springerville PV spectrum and that of the much larger PV array. The highest frequency in the spectra is governed by the Nyquist frequency for the temporal resolution of each data set (1 minute for the PV data, 5 for the solar thermal data, and 15 for the wind data).

2.3.2 Cost of Variability of Solar Thermal, PV, and Wind

The average cost of variability of the Springerville PV plant using average energy production levels to schedule q_h and 2010 CAISO prices is \$11.0/MWh. For the 20 MW+ class PV array, the average cost of variability is \$7.9/MWh. For the Nevada Solar One (NSO) thermal plant, the average cost of variability is \$5.2/MWh (23% capacity factor, but as noted previously, solar thermal plants have a significant thermal inertia that smoothes their power output). Using Katzenstein and Apt's optimization method the cost of variability for the NSO plant is \$4.7/MWh (within 6% of my method using the average q_h). This forecast result confirms the hypothesis that the cost of variability for the solar thermal plant ought to be less than that of the solar PV plant since the solar thermal plant's thermal inertia allows it to continue to produce electricity during cloudy periods. As a comparison, the average cost of variability of 20 ERCOT wind farms using the same price data is $4.3/MWh, with a range between $3.5/MWh and $6.2/MWh. Variability costs of wind were on average lower than that of solar thermal, despite the opposite trend appearing in Figure 4, because solar energy incurs all variability costs during the day when electricity prices are highest. Wind turbines continue to produce energy at night, when electricity prices are lower (Appendix 2F).

The average price of power in the southern CAISO region in 2010 was $42/MWh. Variability cost as a percentage of the price of power varies significantly across power sources (Table 2-4). The average cost of variability per megawatt of installed capacity (Table 2-4) is consistent with the observed variability characteristics (Figure 2-4).

Table 2-4. Cost of variability of solar PV, solar thermal, and wind and the average price of electricity in the CAISO zone or region

	Solar thermal (NSO)	**ERCOT wind**	**Solar PV (Springerville, AZ)**	**Solar PV (20 MW+ class)**
Avg cost of variability per MWh (2010)	$5.2	$4.3	$11.0	$7.9
Avg hourly cost of variability per MW capacity (2010)	$1.2	$1.4	$2.2	$2.0
Avg cost of variability per MWh (2005)	$5.9	$5.0	$12.6	$9.9
Median cost of variability per MWh (2010)	$0.0	$2.2	$0.3	$0.2
Standard deviation cost of variability per MWh (2010)	$15.2	$9.0	$31.0	$18.5
Skewness of cost of variability per MWh (2010)	$12.4	$13.4	$19.2	$10.0
Variability cost as a percent of total cost of power (2010)	11.9%	10.2%	26.5%	18.9%
Capacity factor (or average capacity factor)	23%	34%	19%	25%

The majority of the variability cost consists of charges for balancing energy for all plants considered (Table 2-5). The average energy costs in 2010 were higher than the average regulation costs by nearly a factor of eight (Table 2-1).

Table 2-5. Cost of variability breakdown between energy and regulation charges

	Energy costs	Regulation costs
Springerville Solar PV	69%	31%
20 MW+ Solar PV	65%	35%
NSO Solar Thermal	69%	31%
Wind (average)	73%	27%

Based on sub-array data from the 20 MW+ class PV array, I conclude that the size of an array does not have much influence on its variability cost per unit of energy delivered. The average cost of variability of a sub-array with one-sixth the capacity of the full sized array was $8.2/MWh, compared to $7.9/MWh for the full sized array.

2.3.3 Cost of Variability and CO_2 Displacement

One of the goals of an RPS is to reduce CO_2 emissions by replacing fossil fuel generation with renewable energy. By calculating the hourly marginal emissions factors using the method described in Section 2.2.3 I can calculate the cost of variability in terms of emissions avoided. I note that this measurement is only part of the total cost of emissions avoided when considering renewable energy. Table 2-6 contains the average MEF and average cost of variability per ton CO_2 displaced for each generating unit.

Table 2-6. Average marginal emissions factors and cost of variability per unit emissions

Facility	Average marginal emissions factor (tons CO_2/MWh)	Average cost of variability per ton CO_2
20 MW+ Solar PV	0.56	$33
Springerville Solar PV	0.47	$40
Wind (average)	0.51	$25
NSO Solar Thermal	0.48	$15

As a comparison, Dobesova et al. report the cost of abatement using wind power for the 2002 Texas RPS to be $56 per ton CO_2 ($70 per ton CO_2 in 2011 dollars), not including any costs of intermittency or variability.[7] My result suggests that variability may increase the cost of CO_2 abatement using wind power by a third.

2.3.4 Policy Implications and Discussion

I show through a power spectral analysis of observed data that solar thermal generation is less variable than either wind or solar PV at periods of less than approximately three hours (frequencies greater than ~10^{-4} Hz). The low variability of solar thermal power compared to wind and PV is caused by the thermal inertia: solar thermal can continue producing electricity from the heat in its working fluid during cloudy periods while solar PV cannot. Variability in wind power output is caused primarily by changes in wind velocity, which are more gradual than changes in cloud cover, but traditional wind turbines do not have the inertial capability to continue producing electricity during any but the briefest calm periods. I find that the cost of variability is greatest for solar PV generation at $7.9-11.0 per MWh, less for solar thermal generation at $5.2 per MWh, and lowest on average for wind at $4.3 per MWh. Variability adds $15/tonne CO_2 to the cost of abatement for solar thermal power, $25 for wind, and $33-$40 for PV. These methods can be applied to any variable energy source to calculate the costs of variability and CO_2 abatement.

These results suggest that not all RE technologies should be treated equally in terms of variability charges. The Federal Energy Regulatory Commission (FERC) proposes in its Docket "Integration of Variable Energy Resources" to charge renewable energy resources a per-unit rate for regulation services related to the variability of generation.[9] The Docket states that ISOs may use the same rate they charge utilities for load variability in Schedule 3. FERC envisions that individual transmission utilities can apply to charge different rates as long as they "demonstrate that the per-unit cost of regulation reserve capacity is somehow different when such capacity is utilized to address system variability associated with generator resources".[9] Based on these results, I note that a flat rate under the Docket's Schedule 10 would advantage certain variable generators at the expense of others. One principle that the Docket mentions is "cost causation," or fairly determining a rate based on evidence that the rate is based on real costs. In order to avoid creating market biases, utilities can use methods like ours to determine how each variable generator contributes to total variability cost in its service area. Adopting proposals for intra-hourly scheduling would also help ISOs reduce the cost of RE variability.

Renewable energy generators with lower variability costs require fewer ancillary services for support. Ancillary services often are supplied by gas-fired plants that can ramp up and down quickly. However the quick ramping of the current generation of these plants can increase emissions of NOx, a criteria air pollutant.[10] ISOs and those implementing solar power generation mandates can use the method described here to compare unpriced costs of variable electricity generating technologies.

2.4 Appendix 2A: Forecasts

Running the simulation with forecast data illustrates how the cost of variability can change without a perfect forecast. Here I present a method by which forecast data could be used to develop a likely range for the cost of variability. Because commercial forecast data were not available, I use NREL's System Advisor Model (SAM) as a proxy.

I simulate a forecast of the two data sets using NREL's SAM. SAM takes inputs from different types of renewable energy facilities and climate data, and uses that to simulate the outputs of a typical year of operation. However, SAM is meant to give developers and researchers a general idea of typical outputs of a prospective power plant, and not to make precise forecasts of actual annual output. Because of that, the hourly energy output data from the SAM tool was much less accurate than data that could be produced by today's forecasting techniques. The climate input data, including typical meteorological year (TMY) files or individual year files from 1998-2005, comes from NREL's Solar Prospector.[11] I used individual year data from 1998-2005 to simulate a forecast for each location, and then averaged the forecasted electricity outputs.

I have made the following alterations to Equation 2-1 to accommodate using forecast data for hourly energy scheduling:

Equation 2-6

$$\text{Variability Cost}(h) = \sum_{k=1:n} |\varepsilon_k| P_h / n + P_{up,h} \left| \min\left\{ \begin{array}{c} 0 \\ \min(\varepsilon_k) \end{array} \right\} \right| + P_{dn,h} \left| \max\left\{ \begin{array}{c} 0 \\ \max(\varepsilon_k) \end{array} \right\} \right|$$

In case the observed minimum power output is greater than the scheduled hourly energy, q_h, Equation 2-1 would have calculated a negative cost for up regulation, and vice versa if the observed maximum power output for the hour is less than q_h. Equation 2-6 would make the cost of up or down regulation in those cases zero.

The figures below show a comparison of the SAM output and the actual output for NSO and Springerville. The SAM outputs were normalized so that the total energy produced in the year is equivalent for the actual output and the SAM forecast. The SAM forecast for NSO was shifted one hour behind to match the actual NSO output. The mean error between the SAM forecast and the actual production of NSO is 8.2 MW, or 10.9% of its capacity. For TEP, it is 0.32 MW, or 6.4% of its capacity.

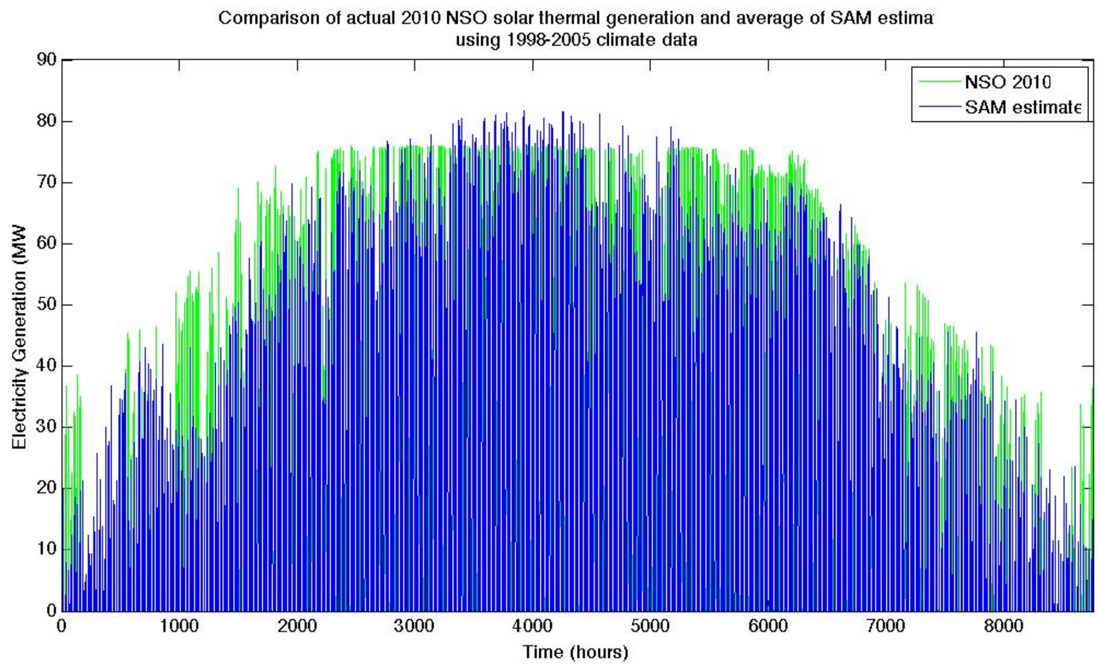

Figure 2-5. Comparison of actual and forecast NSO hourly electricity generation data

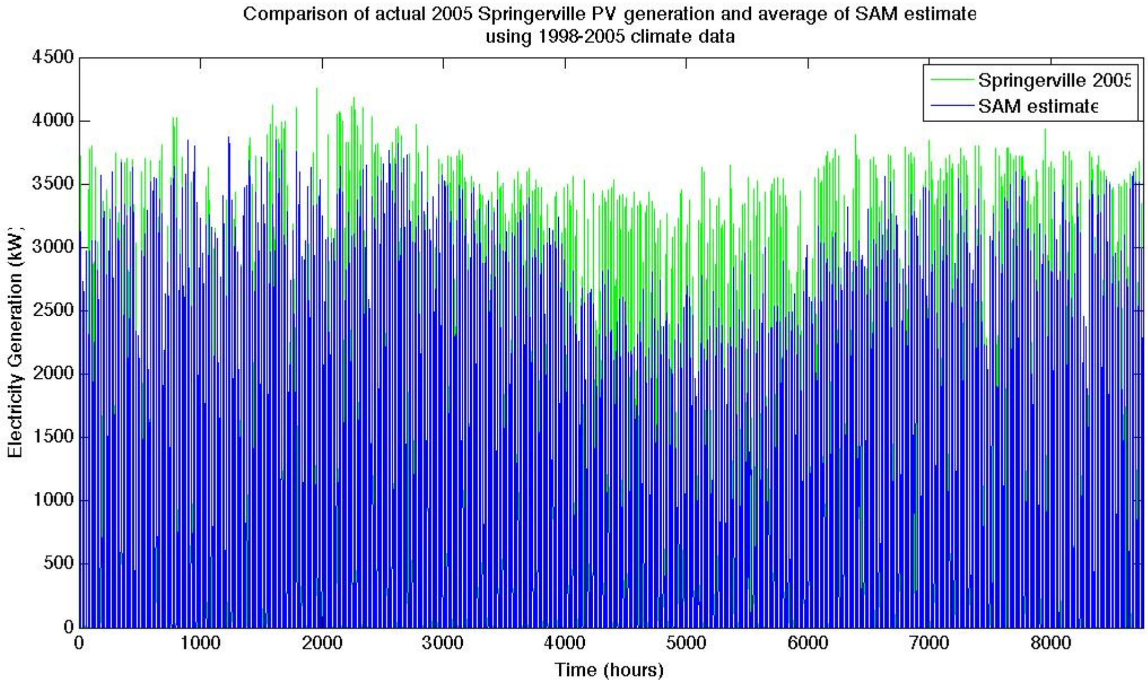

Figure 2-6. Comparison of actual and forecast TEP hourly electricity generation data

Using SAM to simulate an average year of operation, the cost of variability for the thermal and PV plants were \$24/MWh and \$23/MWh, respectively (Table 2-7).

Table 2-7. Cost of variability of solar PV and solar thermal and the average price of electricity in the CAISO zone or region

	Nevada Solar One Solar thermal	Springerville, AZ Solar PV
Cost per MWh	\$5.2	\$11.0
Cost per MWh using forecast simulation (normalized)	\$24.0	\$23.0

I note that the large difference between the perfect information cost of variability and forecast cost of variability, especially for solar thermal, is likely larger than it would be using actual forecast data. Real forecast data of solar PV and solar thermal facilities will be necessary to determine the real cost of variability of each technology. I think that the solar thermal variability and intermittency costs are likely to be lower than those of PV when real forecast data are used, and that SAM energy output estimates are less accurate for solar thermal than they are for PV.

2.5 Appendix 2B: Seasonality of the Cost of Variability

Wind and solar power availability varies on seasonal frequencies in addition to the shorter frequencies analyzed in this paper. I have calculated two seasonal costs of variability for each plant, one for winter (defined as January 1-March 21) and one for summer (defined as June 21- September 21). Table 2-8 summarizes the results.

Table 2-8. Summer and winter costs of variability

	Summer		Winter	
	Average cost of variability per MWh	**Standard deviation of cost of variability per MWh**	**Average cost of variability per MWh**	**Standard deviation of cost of variability per MWh**
NSO	\$3.9	\$8.3	\$6.2	\$19.6
Wind	\$4.9	\$8.4	\$4.5	\$6.8
Springerville PV	\$12.6	\$37.4	\$13.7	\$26.2
20 MW+ PV	\$7.2	\$11.4	\$9.0	\$17.3

There is a marked difference in the cost of variability of the solar thermal (NSO) plant between summer and winter. On average, the cost of variability in winter is 60% higher than it is in the summer. The cost of variability of the two solar PV plants is also higher in winter than in summer, but not by as much as the solar thermal plant: 25% for the 20 MW+ PV plant and 8% for the Springerville PV plant. The cost of variability of the wind farms in summer is 9.5% higher than in winter.

2.6 Appendix 2C: Effect of Period Between Power Measurements on Cost of Variability

If the power output data from the renewable plants is averaged over long time intervals, the apparent variability and resulting computed ancillary service cost will be reduced. I find that interval between power measurements slightly reduces the measured cost of variability, but does not change conclusions drawn from the results using 5 and 15 minute averages compared to 1 minute data (Table 2-9). I also note that the measured cost of variability can vary significantly year-to-year (Table 2-1).

Table 2-9. Average cost of variability using 1-, 5-, and 15-minute intervals

	NSO	Wind	Springerville PV	20 MW+ PV
1-minute	-	-	$11.0	$7.9
5-minute	$5.2	-	$9.7	$7.1
15-minute	$4.6	$4.3	$7.8	$6.0

2.7 Appendix 2D: Effect of Intra-hourly Scheduling on Cost of Variability

Many ISOs are considering implementing intra-hourly scheduling to take advantage of updated forecasts for variable generation and load. I calculate new costs of variability for the different technologies if they were able to schedule their generation twice each hour.

Table 2-10. Intra-hourly Scheduling Cost of Variability

Plant	Average cost of variability ($/MWh) with intra-hourly scheduling	Average cost of variability ($/MWh) with hourly scheduling
NSO	$2.5	$5.2
Wind	$2.2	$4.3
Springerville PV	$7.8	$11.0
20 MW+ PV	$5.2	$7.9

2.8 Appendix 2E: Description of Solar Technologies

Solar photovoltaic technology uses energy from sunlight to create electricity by exciting electrons on a photovoltaic material such as silicon.[12] Solar thermal generation also uses the energy of the sun to create electricity, but instead of exciting electrons, reflecting mirrors focus sunlight on rows of tubes containing a working fluid. The heated working fluid runs through a heat exchanger, creating steam to generate electricity.

2.9 Appendix 2F: Hourly Cost of Variability for Solar Thermal and Wind

The annual average cost of wind variability is lower than that of solar thermal, despite its higher variability (as seen on the power spectral density graph) because wind displays a significant amount of variability at night, when electricity prices are generally lower.

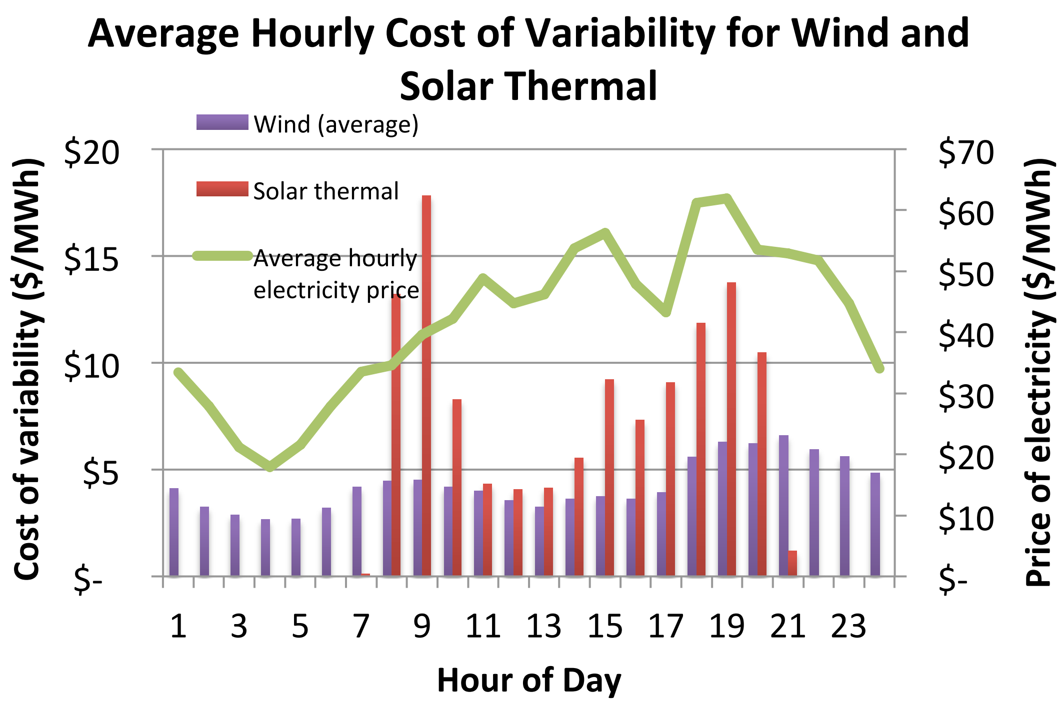

Figure 2-7. Average hourly cost of variability for wind and solar thermal power

3. Distribution Grid Reconfiguration Reduces Power Losses and Helps Integrate Renewables[b]

3.1 Introduction

A reconfigurable network can change its topology by opening and closing switches on power lines. Distribution network reconfiguration is interesting because it allows the grid to operate with lower resistive losses or transmit more power from distributed generation than in static configurations, by dynamically changing its topology in response to changes in load and distributed generation. This technique has been employed in Portugal and other EU countries, and experimentally in the U.S.[c]

Some distribution companies have added or are planning to add significant amounts of distributed generation (DG), such as solar, wind, or natural gas microturbines to their networks. Because of the variability of wind and solar, these networks may experience severe fluctuations in generation. Here I examine whether the loss-minimizing configuration of the network could change depending on the output of wind or solar generation. I also examine whether reconfiguring the network could maximize the use of renewable generation by reducing wind or solar curtailment that would otherwise be necessary due to the finite capacity of the lines and bounded voltages of the nodes. My research contributes to the field of network reconfiguration because it uses real load, wind, and solar generation data, wind forecasts, and prices to calculate reductions in power losses and costs over time.

Reconfiguration is important because sometimes changing the topology of an electrical network reduces operational power losses.[14-17] A network operator might also avoid a voltage or line capacity violation by reconfiguring the grid topology: by changing the electrical path of least impedance, lines transmit more or less electricity and nodes receive power at different voltages.[18] Reconfiguration can also assist distribution

---

[b] Significant portions of this chapter appear in: Colleen Lueken, Pedro Carvalho, Jay Apt. 2012. *Distribution Grid Reconfiguration Reduces Power Losses and Helps Integrate Renewables.* Energy Policy: Vol. 48, pp. 260-273. DOI: 10.1016/j.enpol.2012.05.023.

[c] In the U.S., line switches called reclosers are used as circuit breakers to isolate faults, but I am not aware of any current application of switches used to reduce operational losses. In the 1980s, Oak Ridge National Labs conducted an experiment on a distribution grid in Athens, TN that included reconfiguration. However, they did not experience significant loss reduction.[13]

network operators with service restoration after an outage[19] and with avoiding service interruptions and associated penalties.[20, 21]

When there is DG in a network, reconfiguration can also lower losses and prevent voltage or current violations that the DG might have otherwise caused.[22, 23] If the DG produces power at a rate near that of the demand of the system, then the minimum loss configuration will accommodate the DG as if it were the main power source of the grid. This will likely be a different configuration than when most of the power is coming from the high voltage grid, especially if the DG is located far from the high voltage connection. When the DG introduces more variability, as is the case with wind turbines or solar photovoltaic (PV), the potential for loss reduction through reconfiguration is even greater due to a frequently changing distribution of load over the grid topology. Recent work has shown that reconfiguration can reduce losses of a network with distributed solar PV [24] and wind,[25] but this work does not use time series data.

Due to daily and seasonal variations in load, reconfiguring the distribution network at various intervals throughout the day and year can increase the efficiency of the grid by reducing power losses. Previous work has shown that reconfiguration throughout a day decreases power losses.[26, 27] Also, researchers have extended the analysis of loss reduction to include cost savings.[28] My research extends the application of real load and price data to reconfiguration by using 2008-2010 Electric Reliability Council of Texas (ERCOT) load and price data,[29] wind data and forecasts from a Great Plains wind farm (supplied on the condition of anonymity), and solar PV generation data from a utility-scale array in Arizona[d]. The characteristics of real renewable generation, load, and price data are not easily modeled by simple distributions, so the use of actual data is a required step in determining if distribution network reconfiguration is likely to lead to practical loss reductions.

Another branch of the literature on distribution network reconfiguration deals with algorithms to search for the lowest-loss radial configuration. Researchers have explored

[d] Solar data (two years of data from the 5 MW Springerville Arizona array) comes from Tuscon Electric Power.

the use of evolutionary algorithms[30, 31] as well as genetic algorithms to find efficient configurations.[32-34] Other techniques used include particle swarm optimization,[35, 36] simulated annealing,[37, 38] and decomposition.[39] Rather than use one of these algorithms to solve for the lowest-loss configuration in each time interval, I take advantage of the small size of the test distribution network and calculate results for each plausible radial configuration and choose the one with lowest losses, or alternatively the one that results in the smallest curtailment of wind. The aim is to determine the approximate magnitude of loss reduction or increase in DG accommodated, and to examine the sensitivity of the result to the time interval between reconfigurations.

This work is new because I explore the loss- and cost- reducing benefits of network reconfiguration at different frequencies over months or a year, taking forecasts into account. I look at whether a grid operator can accept more power from a wind or solar PV plant over a year with reconfiguration than with a static network, and examine the penetration level of wind and solar power at which reconfiguration begins to make a difference. I also explore the return on investment of reconfiguration technology.

3.1.1 Summary of Results

I find that grid operators can reduce their resistive line losses as well as the cost of losses by 10-15% through reconfiguration when solar PV provides ~30% of the energy. A network with a 50% penetration of wind may be able to reduce losses using reconfiguration by 30%; smaller benefits from reconfiguration are observed with less than ~50% of system energy supplied by wind. In a scenario without DG, reconfiguration does not significantly reduce losses, but different base configurations have significantly different losses throughout the year. With perfect wind information, increasing the interval between reconfigurations from 5 minutes to 60 minutes negligibly degrades loss reduction; increasing it from 60 minutes to 24 hours degrades loss reduction from around 30% to around 20%. When forecasts inform reconfiguration decisions, the resulting savings decrease by 10-15% compared to perfect information (I do not have solar forecast data, so present forecast implications are only for wind). Reconfiguration allows the grid operator to curtail significantly less wind or solar generation than would be necessary without reconfiguration, depending on the magnitude of the DG resource. This benefit begins at about 30% solar PV penetration by total energy, or 70% wind penetration by total energy. The reconfiguration technology has a negative return on investment when considering just loss reduction, but is positive when using reconfiguration to reduce wind curtailment.

3.1.2 Overview of Paper

Section 3.2 describes the methods and data sets, and the limitations that each confers on the results of my analysis. Section 3.3 contains a detailed description of results and Section 3.4 describes sensitivity analyses. Section 3.5 contains the results of an examination of the economics of reconfiguration. In Section 3.6 I present the policy implications of this research. Section 3.7 contains the conclusions I draw from the results of this research.

3.2 Methods

3.2.1 Data

I modeled the distribution network with typical line characteristics for a medium voltage network (Appendix 3C). Load data come from 2008-2010 ERCOT (Electric Reliability Council of Texas) records.[29] For wind data and forecasts, I use data from a U.S. wind farm in the Great Plains (supplied on the condition of anonymity). The data consist of hourly wind power outputs and 84-hour outlook forecasts generated every 6 hours for 2008 and 2009. Due to a change in reporting style, forecasts from only the first five months of 2008 were useable for this research. Solar data came from the 5 MW Springerville array in eastern Arizona. No forecasts for solar data were available. For load forecasts, I use a two-week rolling average of each one-hour interval. For example, to predict the load from 1:00 am – 2:00 am, I average the past two weeks' loads from 1:00 am – 2:00 am.

Prices for the model come from 2008-2010 ERCOT data for the hourly price of electricity.[40]

In addition, I have load profiles for adjacent feeders from the Lisbon, Portugal metropolitan area to characterize the correlation of demand at different nodes over time.

3.2.1.1 Limitations and Assumptions

I use North American data on loads, wind, and prices to gain insight about the Portuguese electricity system, because Portuguese data were unavailable. The Great Plains wind forecasts record an 84-hour outlook for hours *t* through *t*+84 for the first five months of 2008. For the rest of 2008 and 2009, the 84-hour outlook is for hours *t*+3 through *t*+84. Therefore, I only use the first five months of 2008 data for the analysis using the Great Plains wind farm forecasts. This means that for analysis using wind data, the model spans only five months.

3.2.2 Model

A simple model of an electricity distribution network consists of busses representing loads, generators, and high voltage bus connections. Power lines connect the busses, transmitting electricity from sources to sinks. I define a reconfigurable network as one that can change its topology by opening and closing switches on the power lines. In this paper, I further restrict the discussion to radial distribution networks: networks in which each “child” node has only one “parent” node. I use a modified version of the 13-node IEEE distribution test feeder in the model. Figure 1 shows the original IEEE 13-node distribution test feeder. Figure 2 shows the additional lines I add to the network to enable a meaningful reconfiguration investigation. Figure 3 shows the modified network; I removed the transformer between nodes 633 and 634 to simplify the problem, added a distributed generator with fixed P and Q equal to the amount of DG power produced in each interval at node 611 and replaced the voltage regulation transformer between node 650 and node 632 with an infinite bus with fixed voltage and power angle. Figure 4 shows an example of an alternative configuration. For diagrams of all alternative configurations, see Appendix 3A: Configuration Diagrams.

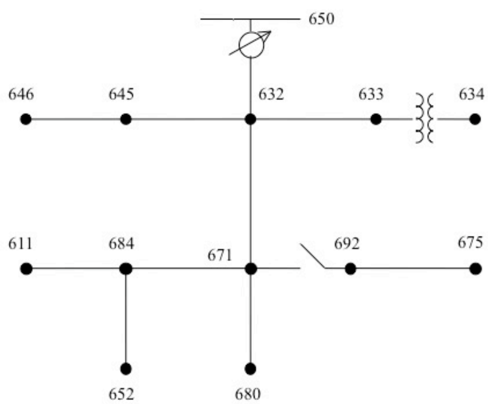

Figure 3-1. Original IEEE 13-node Test Feeder

(circle with arrow represents a generator;
symbol between 633 and 634 is a transformer)

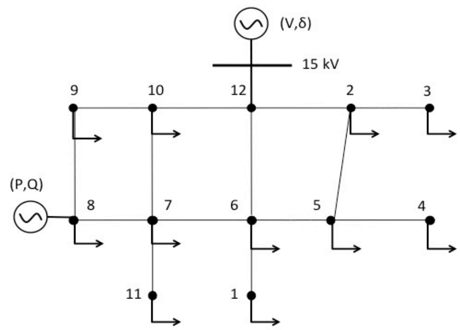

Figure 3-2. Modifications to IEEE 13-node Test Feeder

(generator is replaced by infinite bus; transformer
removed to simplify the model)

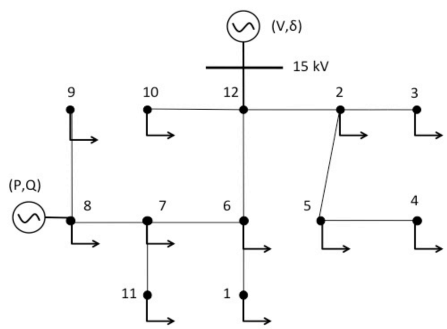

Figure 3-3. Modified 13-node Feeder, base configuration

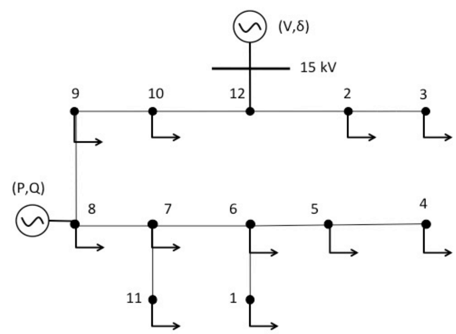

Figure 3-4. Alternative Configuration to IEEE Test Feeder

I use the backwards-forwards sweep method to iteratively solve for the voltages, currents, and total demand of a radial distribution network.[41-46] I chose the backwards-forwards sweep method over the Newton-Raphson power flow solution method because the backwards-forwards sweep method is faster and more reliable than the Newton-Raphson method for radial distribution networks with high R/X ratios.[47] The backwards-forwards sweep method is an iterative power flow solution for radial networks. Starting node voltages are set to a predefined value (for example, 1 per unit), and the source node is considered a fixed voltage source. The first iteration begins at the end-nodes and adds up the shunt and line currents to the branches from child nodes to their network parents. Then the algorithm calculates voltages "forwards" from parent to child nodes accounting for voltage drops for the currents calculated previously and compares the voltages at nodes in iteration v to those in iteration $v-1$. When the difference between the old and new voltages is smaller than a certain threshold for all nodes, the algorithm stops and reports the final branch currents, node voltages, and total network demand.

Configurations with node voltages outside a specified range, or configurations that do not converge[e] within 25 iterations, are discarded. If the objective of the model is minimizing losses, the model compares the losses in the base configuration to losses in each available alternative configuration and selects the configuration with the lowest losses in each time interval. The results of this analysis are presented in Section 3.3 along with a sensitivity analysis in Section 3.4. If the objective is minimizing curtailment of a variable DG resource, the model chooses the configuration with the lowest curtailment in each time interval. The results of this analysis are presented in Section 3.3.2.

There are 60 possible configurations of the model network. By examining the results of all of the configurations in a variety of loading situations, all but 18 were eliminated because they were either never or rarely the loss-minimizing configuration. The difference between loss reduction using all 60 configurations and using only the best 18 configurations is not significant (Table 3-1). To make computation times more efficient, I compare only the 18 most frequent configurations in the optimization. This small solution space obviates the need to employ search algorithm methods to choose optimal configurations. Rather, I can exhaustively search the solution set very quickly.

[e] Convergence in this case refers to the calculation meeting the criteria that the difference in voltage for each node between two iterations does not exceed 0.0001.

Table 3-1. Difference in loss reduction when using 60 and 18 configurations.

Frequency of Reconfiguration (hours)	60 configurations	18 configurations
1	29.53%	29.40%
2	28.18%	28.13%
3	27.36%	27.32%
4	26.69%	26.66%
5	25.93%	25.89%
6	25.41%	25.38%
12	22.09%	22.07%
24	18.92%	18.91%

One output of the model is the percent reduction in losses between the base case scenario (a non-reconfigurable grid) and the scenario with switching at specified intervals. The model considers losses in three scenarios (Table 3-2).

Table 3-2. Model definitions for line losses in different scenarios of solar or wind distributed generation.

Scenario	Definition of loss
No solar or wind	Losses = Electricity drawn from HV grid – Load
Load is greater than solar or wind	Losses = Solar or Wind + Electricity drawn from HV grid – Load
Solar or wind is greater than load	Losses = Solar or Wind – Electricity drawn from HV grid –Load

When the DG produces more electricity than there is demand, the extra electricity is transmitted back to the high voltage grid. The model also considers prices at each hour of operation and calculates how much a utility would save from loss reduction over the course of a year using reconfiguration. The model multiplies the cost of electricity for an hour by the loss savings in the hour to calculate this.

3.2.2.1 Limitations and Assumptions

I divide the test feeder into four zones, each of which contains 2-4 nodes (see Figure 3-5). Total hourly load for the test feeder is determined by dividing the total ERCOT load by 100 to scale the load appropriately for the size of the IEEE test system. Load is divided among the zones by multiplying that quotient by correlated random variables, and then normalized so that the total load of the feeder is still equal to the same fraction of

ERCOT load. I correlate the random variables by using a Cholesky factorization with a correlation of 0.5. Within a zone, I evenly divide the load. In a sensitivity analysis, I examine the effects of using a perfectly correlated data set as well as a data set with no correlation. I also use 24-hour load data from 11 feeders in Lisbon with Bonneville Power Administration (BPA) wind data to simulate realistic feeder correlations (see Appendix 3B: Load Correlation Across the Network).[48] Both analyses support the hypothesis that using an 0.5 correlation with the ERCOT load data is a reasonable assumption.

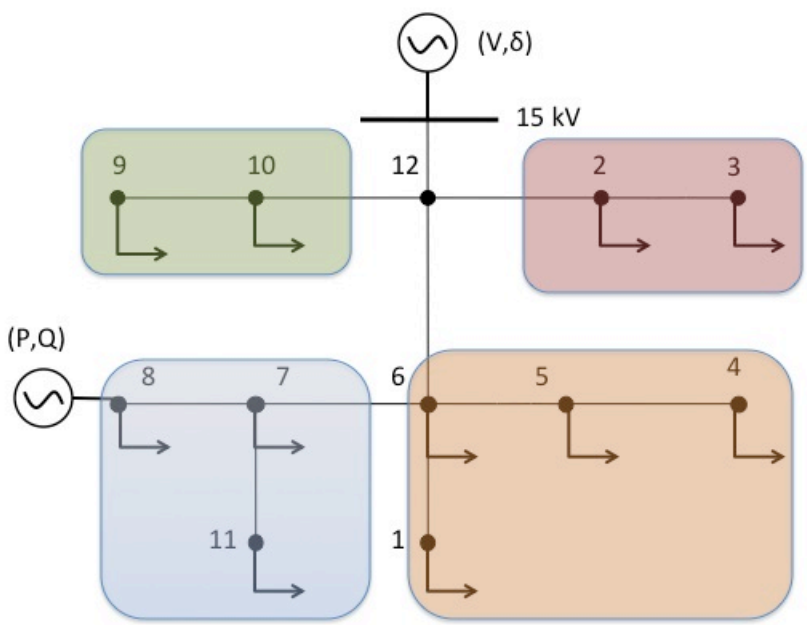

Figure 3-5. Zones of equal load in the test feeder

As this is not a continuous power flow model, the outputs of voltage, current, and total demand are not perfect. This model cannot account for second-to-second variations in demand or wind power output. Rather, it assumes outputs to be constant for at least 5-minute intervals.

I also assume that the high voltage grid connected to the model can accept all of the excess electricity in each time interval without significant changes in voltage magnitude. I assume that all lines can accept the radial flow of electricity in both directions within the constraint of a current limit.

I note that my research considers distribution systems, not the high voltage grid. For the grid as a whole, the N-1 security criterion ensures continuous operation of a system in the event of a single component failure. In a radial distribution system, system operations after a failure of a line or switch are necessarily interrupted for a short period equivalent to the time it takes to detect and isolate the fault and reconfigure the system to an alternative radial configuration. The model does not consider the costs of power interruptions due to switch or line failures.

I get solar generation data from an Arizona 4590 kW solar array. The average output of the array is 867 kW for the 8760 hours in 2005. I scale the array to fit the sample grid by multiplying the output of the array in each hour by a factor between 1.3 (10% penetration by total energy demand) and 13 (100% penetration by total energy demand).

Wind data from the Great Plains wind farm is scaled down to represent a smaller wind farm. I scale down the output of the Great Plains wind farm varies to represent different penetrations of wind in the system. In reality a smaller wind farm would likely have higher intermittency and variability than the full-sized wind farm.

With these assumptions, it is important to ask how applicable these results are to real distribution grids and wind farms. By using months of solar, wind, load data and forecasts, the model more closely mimics a real system than other models that only consider one point in time or a short period of variable load. Also, the levels of loss reduction from reconfiguration in my model correspond to those found by Fisher, O'Neill and Ferris using transmission lines.[49]

3.3 Results: Engineering Analysis

3.3.1 Reconfiguration Can Reduce Losses and Operating Costs of Losses

I find that grids with DG from solar photovoltaic (PV) cells benefit from reconfiguration. Electricity from solar photovoltaic cells is intermittent and variable. The cells produce no electricity at night, and during the day produce electricity at a rate proportional to the angle of the sun in the sky, interrupted by clouds. A network with 20% DG in the form of a solar PV plant may be able to reduce losses using reconfiguration by up to 15%; when DG penetration reaches 30% the network may be able to reduce losses by up to 18%. For penetrations higher than 30%, line current violations occur frequently and it becomes more beneficial to focus on curtailment reduction than loss reduction (Section 3.3.2).

A network with 50% wind penetration can reduce losses by approximately 30%, and similarly reduces the cost of losses by ~ 25%, by using reconfiguration. Analysis of load and price data from 2008-2010 shows that loss and cost reduction fall within a small range. The loss reduction benefits from reconfiguration degrade for networks with lower than 50% wind penetration by total energy (Figure 3-6). A network without intermittent DG cannot expect to reduce losses significantly with reconfiguration unless the base configuration is not optimal for the power flow.

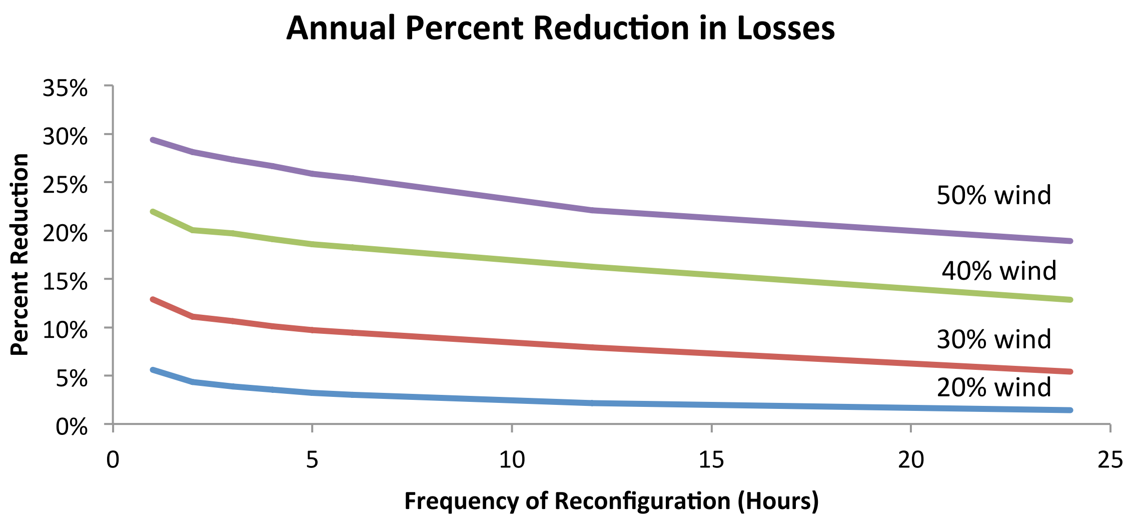

Figure 3-6. Percent loss reduction for different distribution system reconfiguration frequencies for West Texas 2010 load and price data.

Loss reduction potential for wind DG and solar DG at 30% penetration by total energy is similar. The benefit of loss reduction through reconfiguration for wind DG extends to higher penetrations than for solar DG because of the peakiness of the solar curve compared to the wind curve (Figure 3-7). At peak production, the solar array produces about two thirds more power than the wind farm does for equivalent penetrations. The network does not have the capacity to accommodate all of the generation from the solar array, so at higher than 30% penetration, the major benefits from reconfiguration are avoiding line current violations and avoiding solar curtailment (Section 3.3.2).

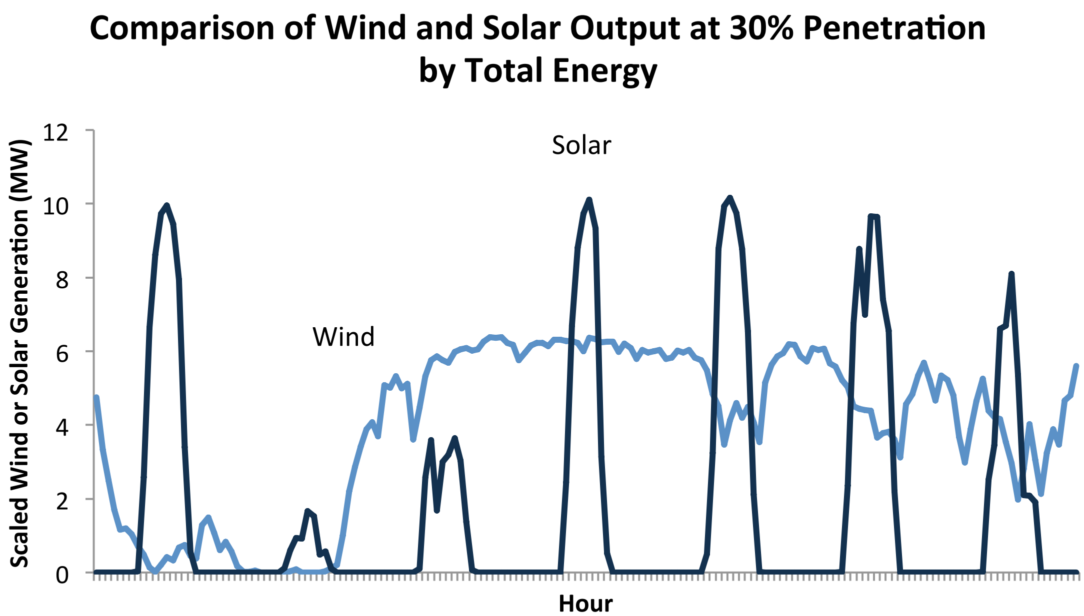

Figure 3-7. Comparison of wind and solar outputs. While the area under the curves is equivalent, the high peaks in solar cause the network to curtail its generation more frequently than for wind. Each tick mark represents one hour.

3.3.2 Reconfiguration Allows Grids to Accept More Intermittent DG

When solar penetration increases, reconfiguration allows the grid operator to curtail less electricity than would be necessary without reconfiguration (Figure 3-8). To simulate solar curtailment, I constrained the power flow solution to reject a solution that exceeds a current limit in one or more of the lines. Rather than curtail all DG in an interval with a line capacity violation, the model reduces the amount of solar or wind by 10% until the capacity violation is resolved or until the solar or wind is completely curtailed in that configuration for that hour. For the system with solar DG, the static network can accept virtually all the electricity from the solar array until it satisfies about 30% of the total load in the system. For the system with wind DG, the static network can accept virtually all the electricity from the wind farm until it satisfies about 65% of the total load in the system. At higher DG penetrations, the reconfigurable network can accept significantly more solar or wind than the static network can.

I also look at the ability of the network to reduce curtailment for a wind farm using reconfiguration. At very high penetrations by total energy (65% and higher), reconfiguration allows the system to accept significantly more wind than a non-reconfigurable system can (Figure 3-9).

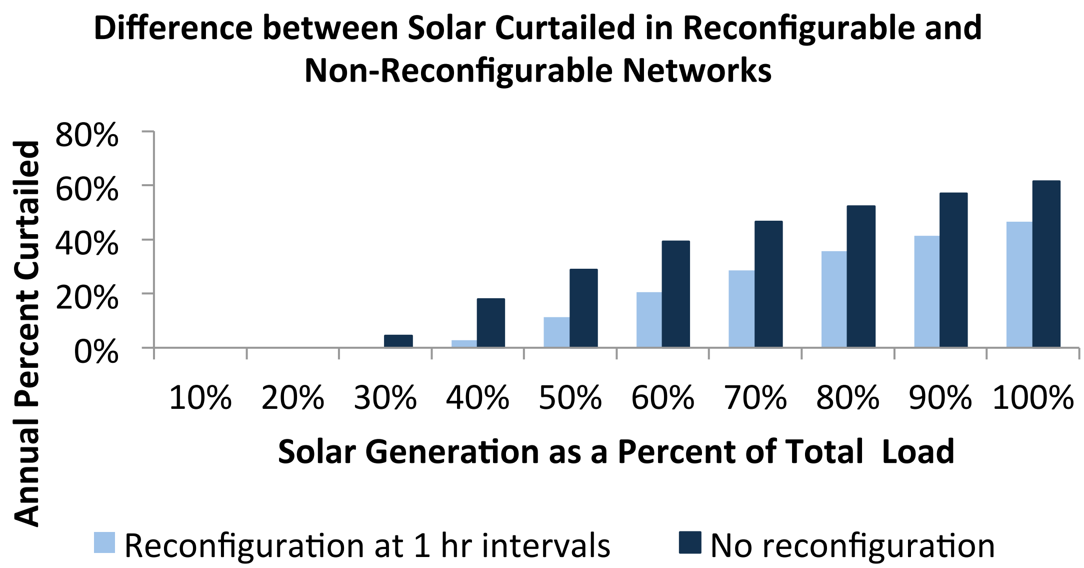

Figure 3-8. Solar curtailment reduction, reconfiguration at 1-hr intervals.

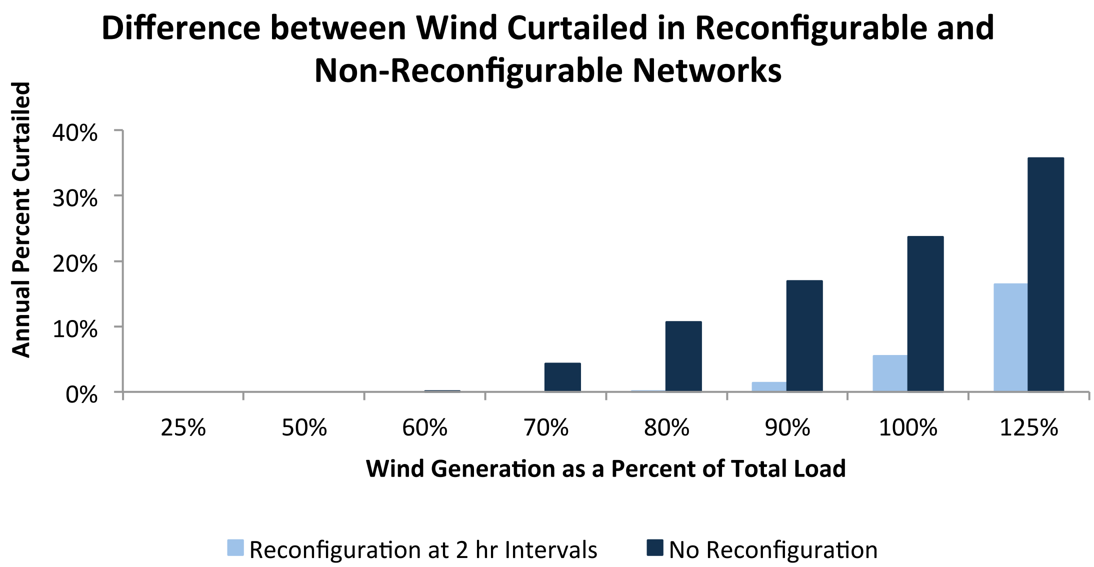

Figure 3-9. Reconfigurable networks require less wind curtailment than non-reconfigurable networks when the generation of wind satisfies about 70% of total demand.

A common way to purchase power from a wind farm is through a power purchase agreement, or PPA. Through a PPA, a load serving entity (LSE), such as my sample grid, agrees to purchase wind produced from the wind farm at a set price for a set period of time. In general, the PPA contains a "take or pay" clause, which requires the LSE to purchase all the power that the wind farm produces regardless of whether there is sufficient load or congestion in the lines.

Under a typical PPA, the grid operator in this model would always be better off maximizing the amount of wind it takes rather than minimizing losses. If the set price in the PPA is much lower than the market price for electricity, the grid operator saves money by reconfiguring to accept more wind. If the set price is much higher than the market price, the grid operator will need to pay it anyway, so it is better to take more wind to avoid purchasing power from the high voltage grid. Penalties for failing to meet a renewable portfolio standard would only strengthen this conclusion. Figure 3-10 shows the potential savings for using reconfiguration to avoid wind curtailment in a network with varying degrees of wind penetration and different PPA set prices. The price for electricity from the high voltage grid comes from ERCOT 2010 price data.[40]

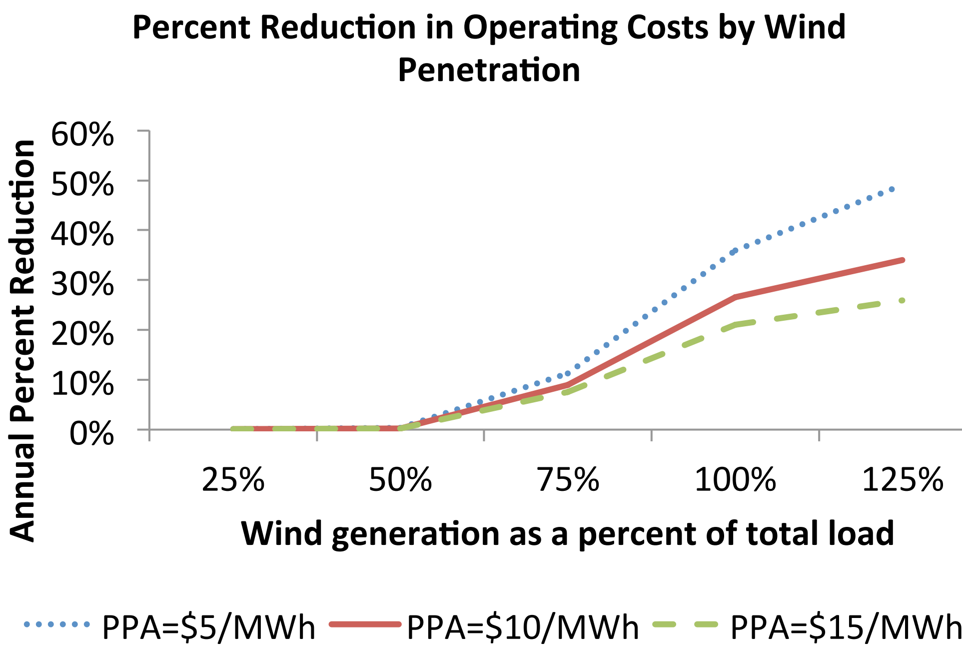

Figure 3-10. Operating cost reductions using reconfiguration to reduce wind curtailment, reconfiguration at 2-hr intervals.

3.4 Sensitivity Analysis

3.4.1 Interval between reconfigurations

Because reconfigurations result in fatigue on the switches, grid operators should limit the frequency of reconfigurations. While reconfiguring less frequently will help avoid wear on the switches, the grid operator sacrifices some of the loss savings due to lower accuracy of wind and load forecasts for longer intervals, as well as the variability of wind and load during longer intervals.

To vary the interval between reconfigurations, I calculate the best configuration using the average load and DG data for the chosen interval. Then using that configuration I calculate actual losses for each hour in the chosen configuration and compare those losses to the base configuration. While it would be possible to further optimize the switching operations through dynamic programming or loosening the constraint that switching operations can only happen at fixed intervals, my method simulates realistic decision-making in distribution grid operations.

By varying the interval between reconfigurations from one hour to 24 hours, I find that, for a scenario with perfect information, the grid operator sacrifices only about 3% of the potential loss reduction by reconfiguring every 6 hours rather than every hour. This means the grid operator may avoid unnecessary fatigue on the switches by reconfiguring less often. Figure 3-11 shows how varying the interval between reconfigurations affects the loss reduction of the system. Even at intervals of 24 hours, the grid operator can reduce losses by around 20% if he could predict with perfect accuracy the loads and wind for the next 24 hours. The percent reduction in the cost of losses follows a similar pattern as loss reduction but is more variable because of the variations of average electricity price in ERCOT in different regions and years (Figure 3-12).

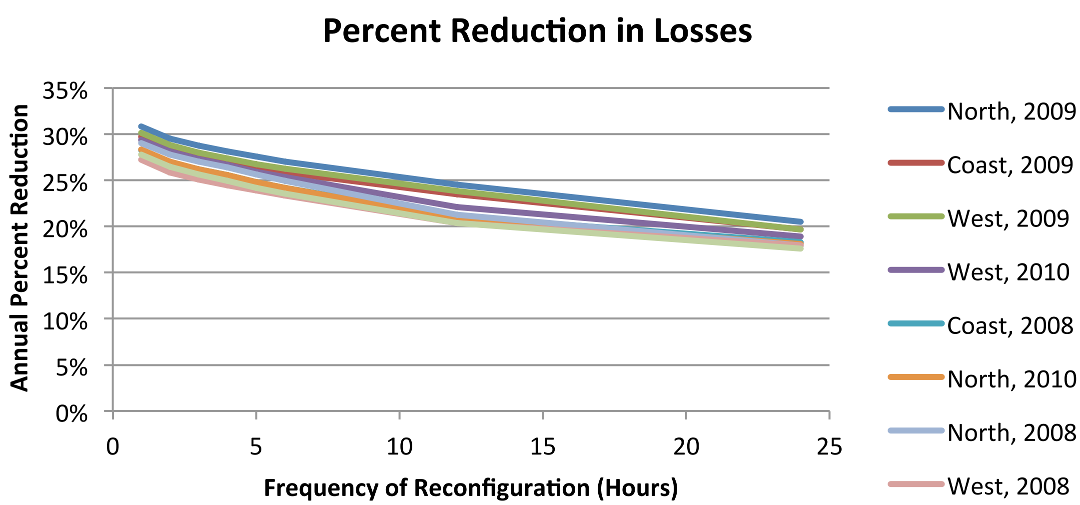

Figure 3-11. Reduction in losses from reconfiguration, using data from different regions and years within ERCOT, 50% wind penetration by total energy.

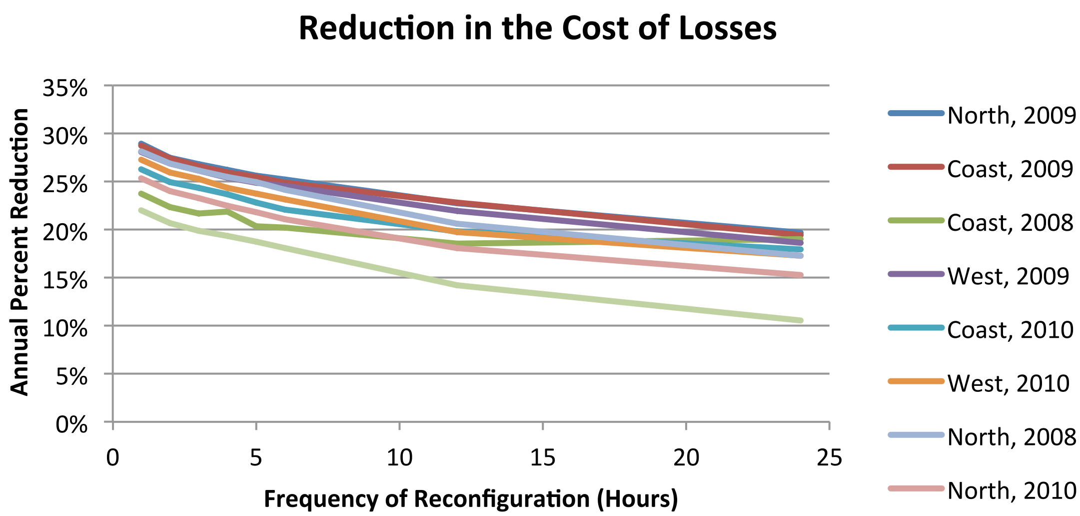

Figure 3-12. Reduction in the cost of losses from reconfiguration, using data from different regions and years within ERCOT, 50% wind penetration by total energy.

3.4.2 Reconfiguration at High Frequencies Does Not Significantly Improve Loss Reduction

As a first analysis, I used 5-minute BPA wind, load, and forecast data to examine loss reduction with reconfiguration. However, the result of varying the frequency of reconfiguration between 5 minutes and one hour shows that there was not a significant difference in loss reduction at frequencies of less than one hour (Figure 3-13). Since reconfiguring more frequently reduces the lifetime of the switches, it is better to choose a lower reconfiguration frequency if the difference in loss reduction is not significant.

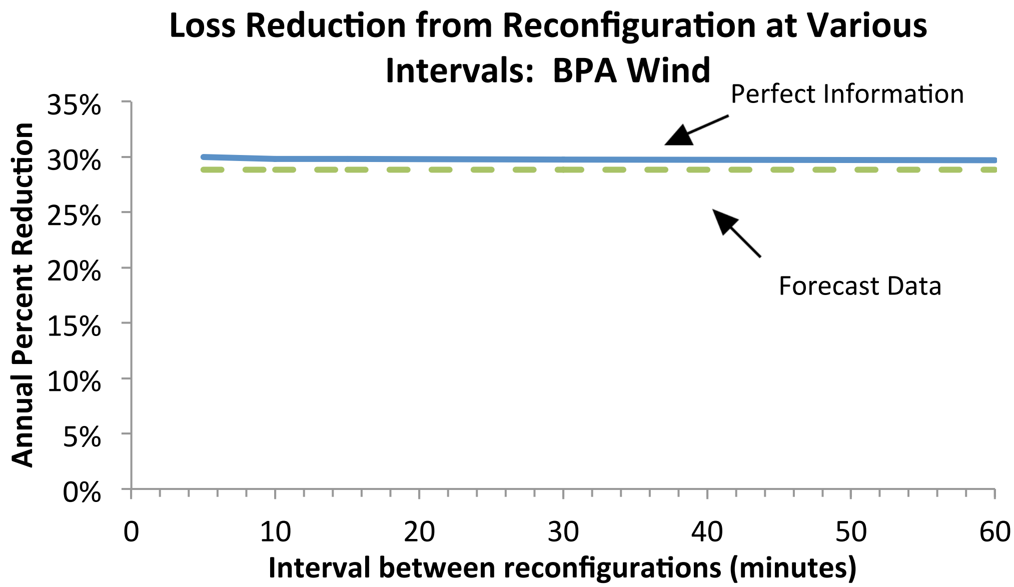

Figure 3-13. Loss reduction from reconfiguration at intervals of less than one hour; 50% wind penetration by total energy.

3.4.3 Reconfiguration Based on Forecasts of Wind and Load

Modeling grid operations without perfect information and comparing the results to an operator who has perfect information shows how the reconfiguration model might operate in a real situation. Using wind power forecast data from a Great Plains wind farm, and reconfiguring at a frequency of one hour, the operator using wind and load forecasts reduces losses by 5% less than the clairvoyant operator (Figure 3-14). When the interval between reconfigurations is larger than one hour, the percent difference in loss reduction between perfect and forecast information does not change significantly. A possible explanation for this is because reconfiguring every 12 or 24 hours already requires a sacrifice in loss reduction (due to variability during the period between reconfigurations), using the forecasts instead of perfect information is not the dominant reason for poorer performance.

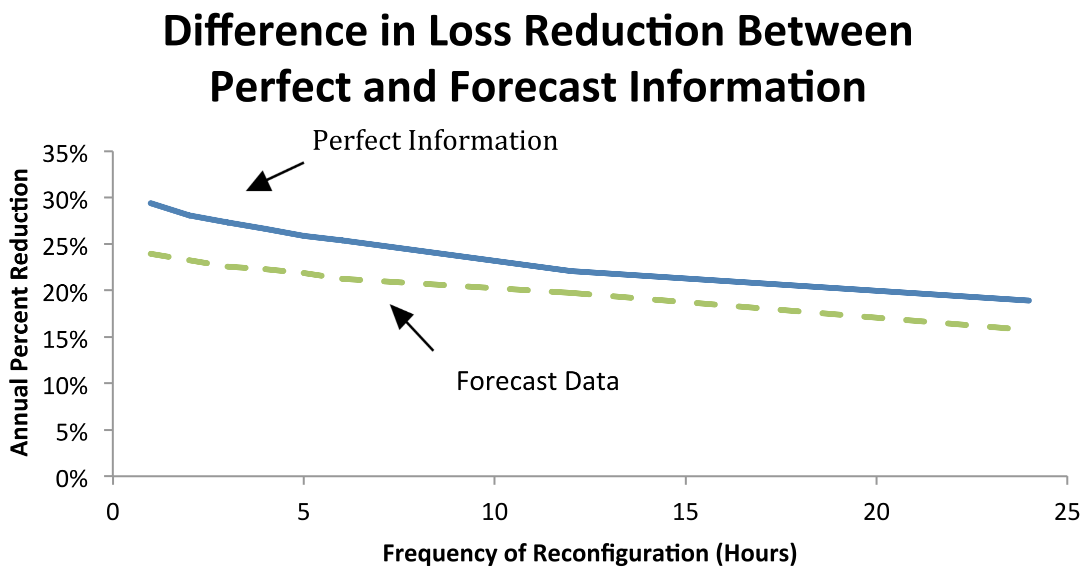

Figure 3-14. Reduction in losses using perfect information and forecasts, West Texas 2010 load data. Wind data from Great Plains wind farm, 50% penetration by total energy.

3.4.4 Changing the Location of the Distributed Generation

Depending on the location of the DG in the network, the potential for loss reduction changes. In this network, a wind farm at node 8 confers the largest potential loss reduction through reconfiguration compared to the static configuration with lowest losses. In contrast, a wind farm at node 1 or node 10 has less potential for loss reduction (Figure 3-15 and Figure 3-16). The same pattern emerges for the DG solar array: the loss reduction potential during a year of operation with 30% solar penetration by total energy is 18%, 11%, and 8 % for an array at node 8, node 10, and node 1 respectively.

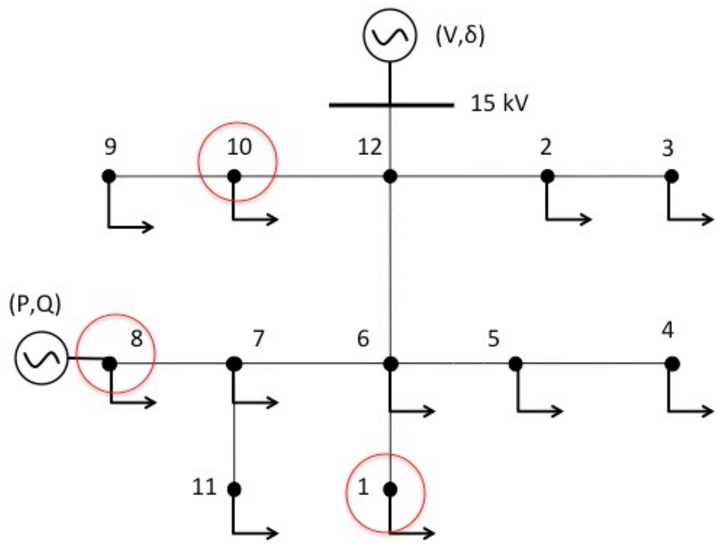

Figure 3-15. Sample network with alternative DG locations circled. Node 8 is the standard location for the wind or solar DG resource throughout this analysis.

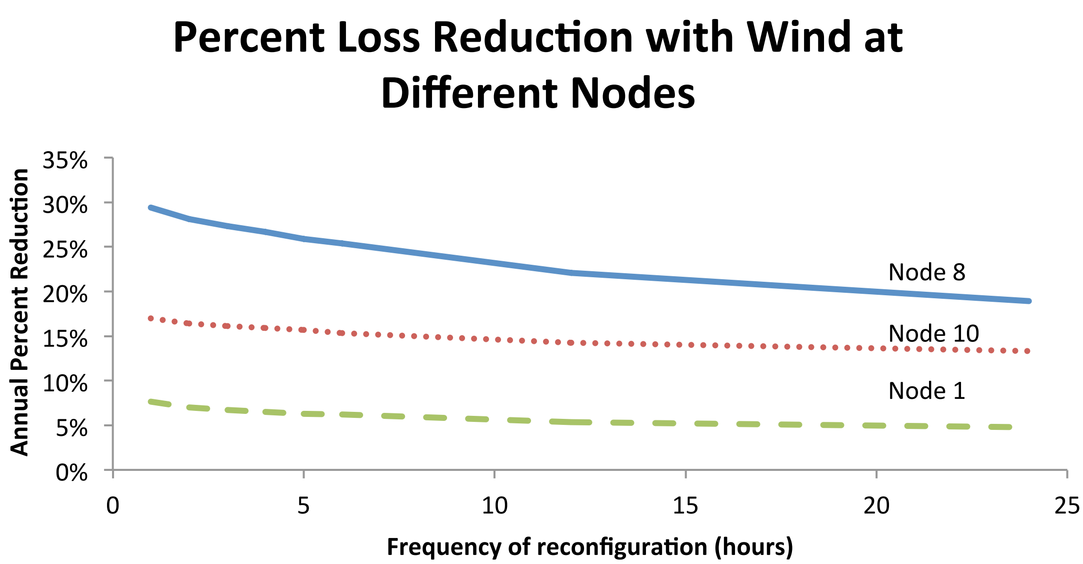

Figure 3-16. Effect of changing the location of the wind farm on loss reduction.

3.5 Results: Financial Analysis

3.5.1 Net Present Value Analysis

The interval between reconfigurations determines the expected lifespan of the switch based on an expected 10,000 actuations per switch. With this information and the capital costs of the switches and remote automation technology, one can calculate the net present value of an investment in reconfiguration technology for the test network. For the NPV analysis and sensitivity analysis I use the values in Table 3-3 and a 20-year outlook.

Table 3-3. Values used in NPV analysis.

Item	Best Estimate	Source
Price of switch	$10,000	[50]
Price of remote actuator	$3,000	(Stoupis, 2010)
Average lifetime of switch and actuator (in actuations)	10,000	(Stoupis, 2010)
Discount rate	10%	

The savings a grid operator experiences depend on how often he reconfigures the network throughout the day. Using the Great Plains wind forecasts and ERCOT load forecasts and price data from 2010, I calculate the annual cost savings for each reconfiguration frequency (Table 3-4).

Table 3-4. Annual cost savings expected through reconfiguration at different intervals. Assumes 70% wind penetration for the wind curtailment scenario and 50% wind penetration for the loss reduction scenario.

Hours between Reconfigurations	Savings per year (forecast, wind curtailment)	Savings per year (forecast, loss reduction)
1	$88,400	$4,700
2	$88,400	$4,500
3	$87,900	$4,400
4	$87,800	$4,300
5	$87,300	$4,300
6	$87,300	$4,100
12	$80,300	$3,700
24	$74,700	$2,900

Based on the annual cost savings and the cost of switch installation and replacement over the 20-year period, Table 3-5 shows the expected NPV of the investment based on the objective of the reconfiguration (avoiding wind curtailment or loss reduction) and the number of hours between reconfigurations. The results do not follow a monotonic trend because reconfiguring at short intervals creates higher savings, but it also results more frequent switch replacement, which adds to capital costs. The result in Table 3-5 shows that the return on investment when avoiding wind curtailment is very attractive, while the investment costs do not outweigh the monetary benefit of using the technology solely for loss reduction. For both scenarios, reconfiguring every 3-6 hours creates the highest NPV.

Table 3-5. Net Present Value Savings from Wind Curtailment Reduction and Loss Reduction, PPA=$10/MWh. Assumes 70% wind penetration for the wind curtailment scenario and 50% wind penetration for the loss reduction scenario.

Hours between Reconfigurations	NPV savings-costs wind curtailment	NPV savings-costs loss reduction
1	$560,000	$(150,000)
2	$610,000	$(110,000)
3	$630,000	$(80,000)
4	$630,000	$(80,000)
5	$620,000	$(80,000)
6	$630,000	$(80,000)
12	$570,000	$(90,000)
24	$520,000	$(90,000)

Although in Portugal and many other EU countries it is common to have meshed distribution networks in urban and semi-urban areas, other networks may require new lines in addition to switches to enable reconfiguration. Typical costs for new lines are listed in Table 3-6.

Table 3-6. Costs of Different Distribution Line Types [51]

	$/km	Cost of adding three lines to test network
ACSR Robin	$29,400	$57,330
ACSR Beaver	$36,400	$70,980
ACSR Partridge	$47,600	$92,820

The costs of new lines do not change the conclusion that using reconfiguration for loss reduction does not create a positive return on investment. It also does not affect the conclusion that using reconfiguration to avoid wind curtailment is a cost-effective use of the automated switches for this network only if the penetration of wind is very high (70% or greater).

3.6 Policy Implications

Reconfiguration reduces losses, making the entire electric power delivery system more efficient. The Energy Information Administration estimates electricity losses account for 6.6% of total energy use in the US electricity sector.[52] If reconfiguration were widely used for loss reduction, a utility with high distributed renewable penetration may be able to postpone building more generation capacity by improving efficiency instead.

Reducing losses and accepting more wind or solar generation imply that reconfiguration may reduce CO_2 emissions. However, more formal investigation taking into account the full portfolio of electricity generation for the grid would be needed to make an accurate assessment of CO_2 reduction potential.

Depending on the market structure in which the grid operates, benefits will accrue to stakeholders in different ways. Grid operators may reduce costs because they have reduced their losses. If the grid operates in a state with a renewable portfolio standard, and reconfiguration allows a grid operator to accept more of a renewable resource because the lines are congested less often, then the grid operator may benefit from purchasing fewer renewable electricity credits (RECs). If the utility has signed a PPA with the renewable electricity plant, being able to accept more of its electricity could save the utility in terms of operating costs. If the grid does not contain wind, grid operators still may consider whether the configuration of their network is optimal for delivering load with minimal losses.

Wind farm or solar PV plant operators not operating under a PPA will benefit if reconfiguration allows the grid to accept wind more often by reducing line congestion. The utility can purchase electricity from the renewable resource more often and the wind farm or solar PV plant operator gets higher revenue.

There is still a need for communication among wind generators, loads, switches, and the distribution control center to facilitate reconfiguration operations over time.

While cost savings may justify investment in reconfiguration for avoiding DG curtailment, there are also economic incentives to invest in efficiency. For example, distribution utilities in BPA can get reductions in wholesale electricity price for implementing efficiency measures (0.25 cents discount per kWh up to 70% of the capital expenditure).[53]

3.7 Conclusion

Using real solar, wind (forecast and actual), load, and price data I show that grid operators may be able to reduce operational power losses and accept more solar or wind generation using reconfiguration. At the current cost of reconfiguration technology, a net present value analysis shows that loss reduction alone is not enough to warrant investment in switches. However, the results show that reconfiguration would allow an LSE to cost-effectively get more value out of a PPA with a wind farm or solar array, if the penetration of the renewable DG in the system is over a certain threshold. Impending Renewable Portfolio Standard requirements would strengthen the argument for using reconfiguration to reduce renewable resource curtailment.

3.8 Appendix 3A: Configuration Diagrams

The following figures represent the different configurations of the network.

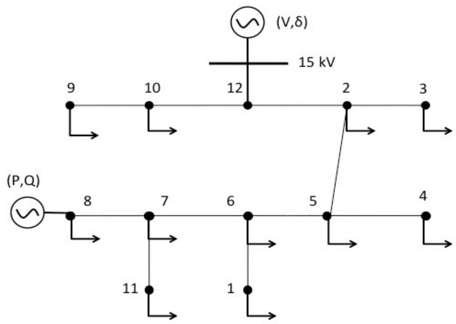

Figure 3-17. Configuration 1

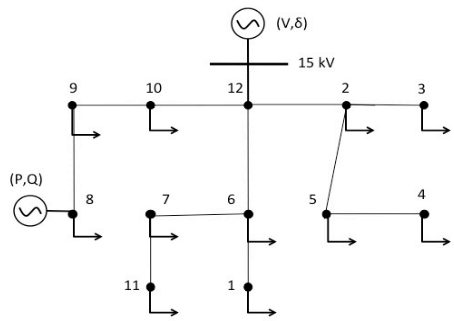

Figure 3-18. Configuration 2

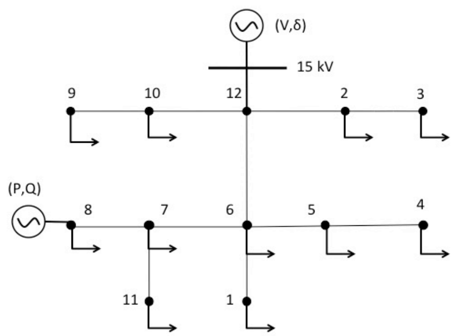

Figure 3-19. Configuration 3

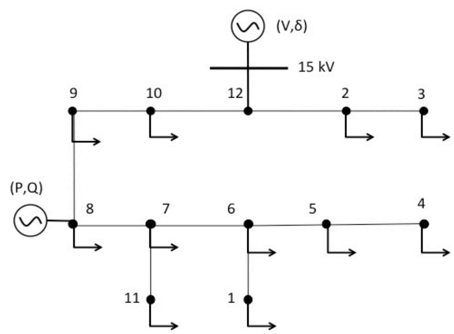

Figure 3-20. Configuration 4

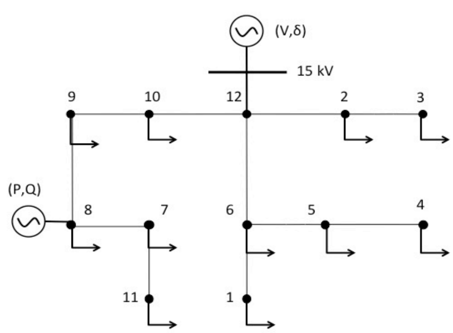

Figure 3-21. Configuration 5

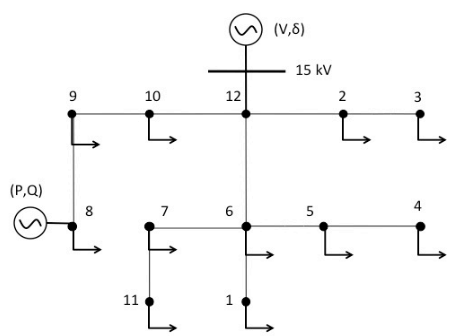

Figure 3-22. Configuration 6

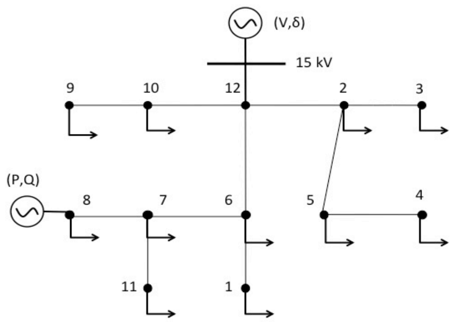

Figure 3-23. Configuration 7

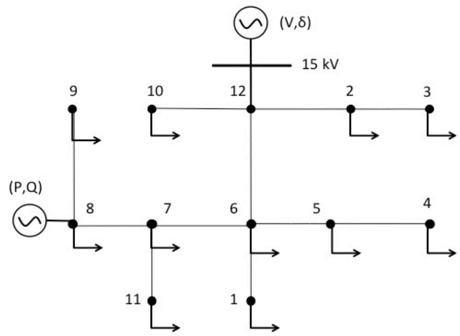

Figure 3-24. Configuration 8

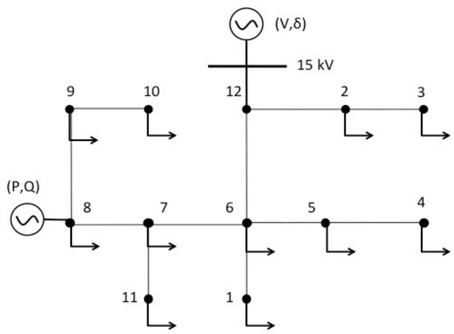

Figure 3-25. Configuration 9

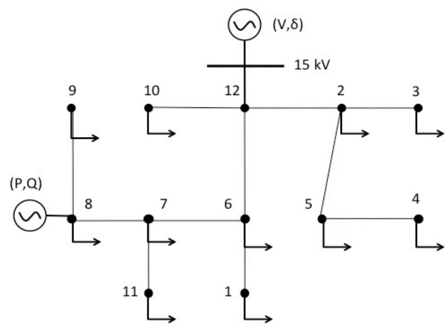

Figure 3-26. Configuration 10

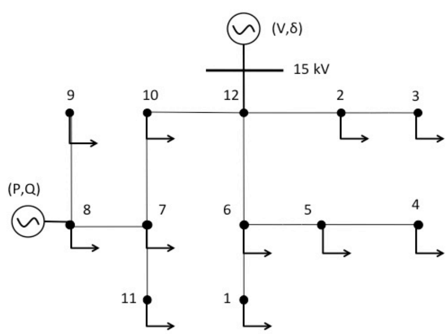

Figure 3-27. Configuration 11

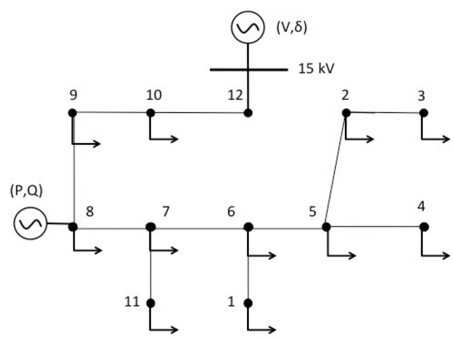

Figure 3-28. Configuration 12

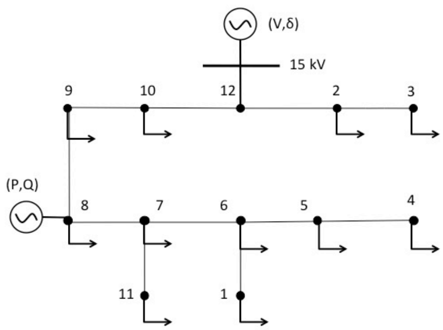

Figure 3-29. Configuration 13

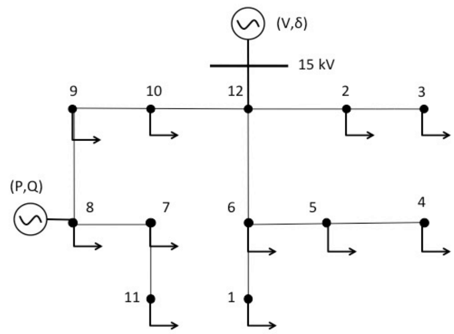

Figure 3-30. Configuration 14

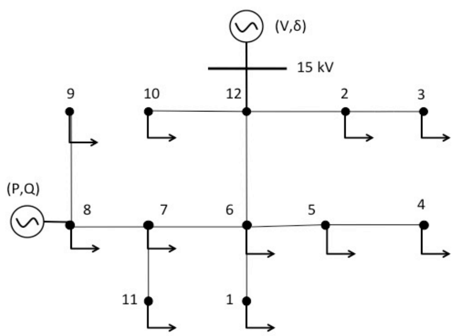

Figure 3-31. Configuration 15

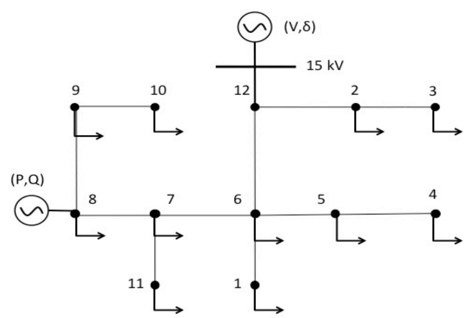

Figure 3-32. Configuration 16

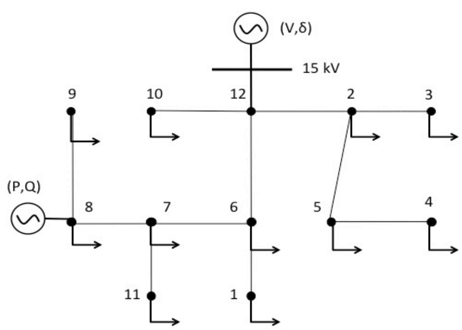

Figure 3-33. Configuration 17

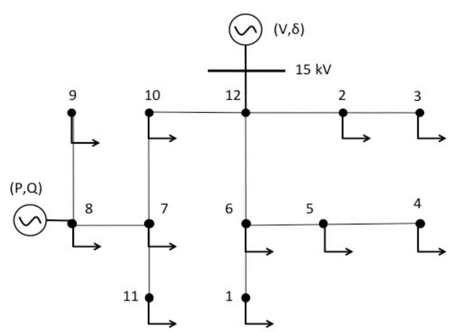

Figure 3-34. Configuration 18

3.9 Appendix 3B: Load Correlation Across the Network

It is important to show that the results of this model are robust given the assumption about distributing load across the different zones using correlated random variables. The first experiment I used to test this was to get real data from feeders in the Lisbon area for a 24-hour period. I normalized the loads by the average load in each feeder so that the demand would be small enough for this model. Since I only had a 24-hour period of data, I simulated adding wind to the model by looping through 365 days of scaled BPA wind using the same day of Lisbon feeder load. The results in Figure 3-35 show that the loss reductions predicted by BPA load at each interval fall within a standard deviation of loss reductions predicted by the Lisbon feeder load, and are only slightly higher than the mean.

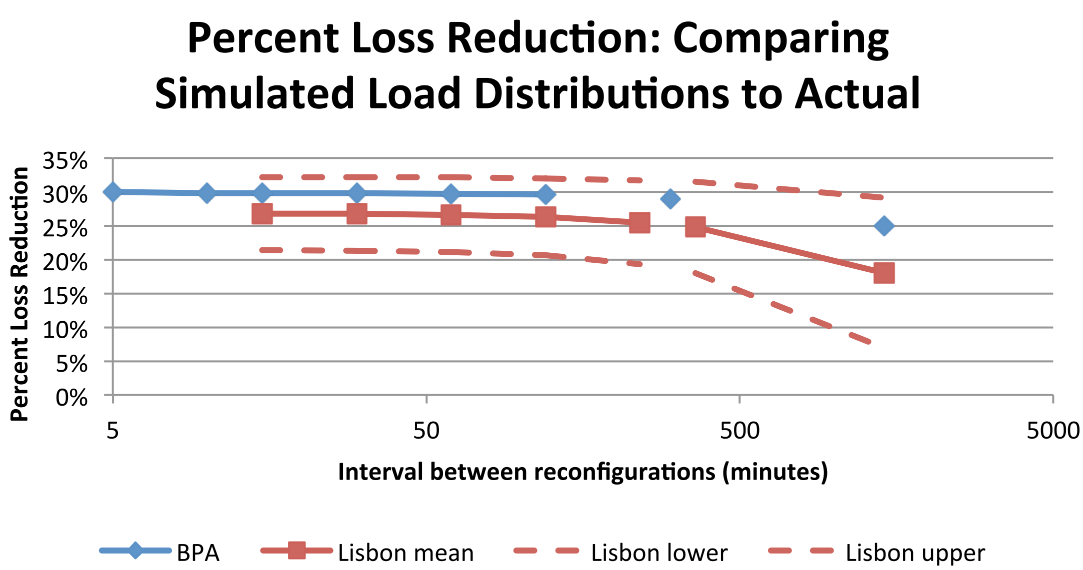

Figure 3-35. Percent Loss Reduction of BPA Load and Lisbon Feeder Load with BPA Wind

A second method I used to verify my assumption was to change the correlation of the random variables that determine the distribution of load across different zones. I bounded the calculation by using perfectly correlated and perfectly uncorrelated loads for each switching interval. The results in Figure 3-36 show that the base correlation (0.5) that I used and perfectly correlated loads behave almost identically; the no correlation scenario loss reductions drop off at large intervals, probably because the variability of the load makes it difficult for a single configuration to minimize losses over a long period of time.

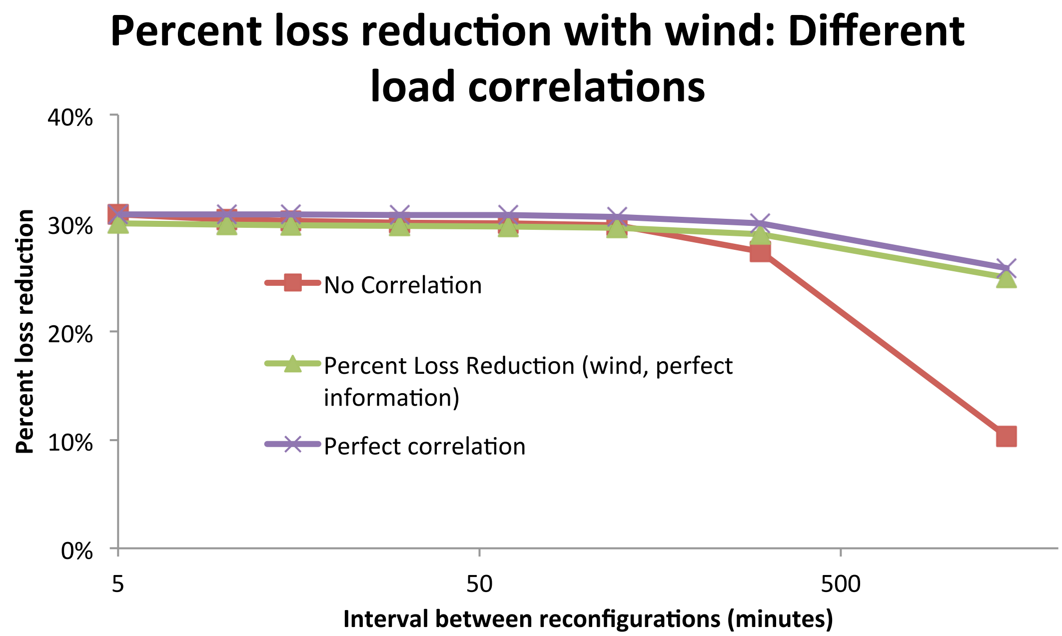

Figure 3-36. Percent Loss Reduction for Different Load Correlations, BPA Load and Wind Data

3.10 Appendix 3C: Model Line Characteristics

Table 3-7. Model line characteristics

Characteristic	Value
Base voltage	15 kV
Line length	0.65 km
Base current (1 pu)	385 A
Max current (1.17 pu)	450 A
Line impedance	0.25+0.35i ohms/km
Line admittance	0.7 kvar/km

4. Market Effects of Pumped Hydro Storage in Portugal

4.1 Introduction

Portugal plans to increase the nation's pumped hydro storage capacity to better integrate wind energy into the electricity system and insulate against price volatility in imported fuel. Most thermal generation and hydropower in Portugal and Spain participate in the MIBEL electricity market, which traded on average 24.6 GWh of electricity per hour in 2011.[54] The maximum energy traded in one hour on the market in 2011 was 37.9 GW. Renewables, small hydro,[f] and some cogeneration operate in a "special regime," receiving feed-in tariffs for power production.[56] To fulfill stringent renewable energy consumption targets, Portugal plans to more than double its current hydropower capacity to 9.5 GW.[57, 58] Of the new hydro capacity, 636 MW will be equipped with storage capability.[58] This increases Portugal's pumped hydro storage capacity by 64%.

Portugal intends for the new storage to balance variable electricity generation from renewable energy and distributed generation.[59] In 2010, Portugal had 3.8 GW of wind capacity, up 360% since 2005.[60] Storage can supplement wind by storing excess electricity at night and discharging during the day, when winds are generally calmer and electricity prices are higher. Portugal is also motivated to develop domestic energy sources such as wind and hydro because it imports all of its coal and natural gas for thermal generation.[60] Because of the large reservoir capacity, pumped hydro can balance variations in generation and load on different time scales, from sub-hourly to more than one week. The new storage capacity will act as both traditional hydropower and pumped storage.[g] Portugal will benefit from traditional hydropower production because it can help the country meet CO_2 emissions reductions targets with a low marginal cost of production. This paper focuses on only the storage aspect of the new investments and the associated costs and benefits of storage.

---

[f] Small hydro generally refers to run-of-river hydropower systems and capacities below 10 MW.[55]
[g] I define traditional hydro as non-pumping conventional dams. A conventional dam becomes capable of providing pumped storage by adding a second dam downstream and pumping capability at the upstream dam. This paper considers only new pumped storage

I examine the effects of new pumped hydro capacity in Portugal on the market price of electricity, consumer expenditures, thermal generator profits, and CO_2 emissions. The size of the new storage capacity compared to the total generation capacity trading in MIBEL is large enough to affect electricity market prices. Three companies plan to build pumped hydro storage facilities in Portugal: EDP, Iberdrola, and Endesa (Table 4-1). Each of these companies also owns thermal generation assets in the Iberian Peninsula (Table 4-2).

Table 4-1. New pumped hydro capacity and owners

Dam	Owner	Capacity (MW)
Baixo Sabor	EDP	170
Foz Tua	EDP	234
Alvito	EDP	48
Gouvães	Iberdrola	112
Girabolhos	Endesa	72

Table 4-2. Coal and natural gas generation capacity for each storage owner.[61–63]

	Coal (MW)	Natural Gas (MW)
EDP	2640	3736
Iberdrola	1253	5893
Endesa	5050	2934

I use a nonlinear optimization approach to model the relationship between price and load in the Iberian Peninsula. I show that the effects of storage on the market change depending on the ownership structure and consequently the operating policies of storage. I show the effect storage ownership has on CO_2 emissions, consumer expenditure on electricity, and thermal generator profits.

Operation decisions of the storage owner vary depending on his incentives. An independent storage owner with no other generation assets will try to maximize profits through energy arbitrage. A storage owner with other thermal generation assets may try to manipulate the market price of electricity with energy arbitrage to drive up profits at the thermal generators. A consumer-owned storage facility would seek to minimize consumer expenditures on electricity. Sioshansi (2010) finds that none of these ownership arrangements creates the socially optimal storage use, which he defines as the sum of consumer surplus, producer surplus and arbitrage profit.[64] This paper calculates the storage operation decisions that result from the actual thermal-generator ownership structure of the Portuguese storage system, and delineates the consequences to consumer expenditure, CO_2 emissions, and thermal generator profits. I compare these results to the independent and consumer-owner cases.

I find that the different operating policies produce different storage use profiles, and consequently have different effects on CO_2 emissions and electricity prices in Portugal. This research goes beyond previous work because it shows the relationship among ownership structure of storage, market prices and CO_2 emissions. It is important that Portugal be aware that thermal generation companies who own storage will increase market price volatility and therefore increase emissions, which is not the outcome from storage investment that Portugal intends.

Finally I examine the cost effectiveness of investment in pumped storage from each ownership perspective. These new dams will receive revenues from producing traditional hydropower and potentially from operating in the ancillary services market in Portugal. My research focuses on just the potential revenues from energy arbitrage. The cost of a pumped storage hydro plant is about 80% greater than an equivalently sized traditional hydro plant.[65] Using that difference, I estimate that the cost of the investment attributable to electricity storage is €660/kW. Even with perfect knowledge of electricity prices, the expected net revenues from arbitrage for an independent storage owner are not enough to create a positive return on investment for the current MIBEL generation mix and prices. However for the consumer-oriented and thermal fleet storage owner, expected profits would create a positive return on investment. As a comparison, I find that an independent storage owner operating under CAISO (California Independent System Operator) prices would see a positive return on investment because of higher price spreads in the CAISO market.

This paper is organized as follows. Section 4.2 contains an explanation of the methods used to complete the analysis, including the data sources, optimization formulations, and assumptions. Section 4.3 contains the results, including the effects of storage on market prices, the potential profit from arbitrage, the effects of storage ownership on consumer expenditures, thermal generator profits, and CO_2 emissions, and a financial analysis of the cost effectiveness of storage. Section 4.4 contains the conclusions and the policy implications of my results.

4.2 Methods

4.2.1 Data

I use 2011 price and market volume data from MIBEL, the Iberian Electricity Market.[66] To model the pumped hydro storage units, I use technical specifications from EDP (Electricidad de Portugal), a Portuguese electricity generation company, and PNBEPH (Programa Nacional de Barragens de Elevado Potencial Hidroeléctrico), the Portuguese organization for hydroelectric power development.[67, 68] Technical specifications for each of the five dams are listed in Appendix 4A. To examine how results translate to other electricity markets, I also run the simulation using price and load data from CAISO in 2010.[69]

4.2.2 Model

Using a nonlinear optimization program to model the storage system, I calculate the changes to consumer expenditure on electricity, thermal generator profits, and CO_2 emissions that result from storage-influenced changes to market prices. I solve the optimization problem using the Tomlab NPSOL solver in Matlab.[70] The amount of energy discharged from or added to the dams in each hour is related to the flow rate of the pump-turbine at each dam, its efficiency, and the head height. Equations 4-1 through 4-3 formalize the three alternative objective functions, and Table 4-6 contains the constraints on the optimization.

I consider three cases: an independent storage owner, thermal generator-owned storage, and consumer-owned storage. The objective function for the independent storage owner maximizes net revenues from electricity arbitrage (Equation 4-1). In the case where one entity owns thermal generation and storage, the owner maximizes arbitrage profits from the storage plus thermal profits (Equation 4-2). Thermal profits consist of the difference between the market price of electricity minus the marginal cost of operating the generator multiplied by the energy supplied by the generator in a given hour. When the market price is less than the marginal cost of operating the generator, the generator does not run. For consumer-owned storage, the objective function minimizes the consumer expenditure on electricity plus the cost of operating the storage system, with the assumption that consumers pay the market price of electricity multiplied by the traded volume of electricity in each hour (Equation 4-3).

Table 4-3. Parameters and their units in the optimization equations

Parameter	Symbol	Unit
Time step index (hour)	i	-
Pumped hydro storage index	k	-
Slope of the price-demand function at hour i	a_i	-
Y-intercept of the price-demand function at hour i	b_i	-
Observed market volume traded in hour i	d_i	kWh
Acceleration of gravity	g	m/s^2
Head of storage unit k in hour i	$h_{i,k}$	m
Number of hours in the optimization horizon	N	-
Marginal cost of operating thermal generator j	r_j	€/kWh
Efficiency of pump in storage unit k	η_k^{up}	-
Efficiency of turbine in storage unit k	η_k^{dn}	-
Maximum flow rates of turbine-pump k	$q_k^{up,max}$, $q_k^{dn,max}$	m^3/s
Maximum power output of thermal generator type j	w_j^{max}	kW

Table 4-4. Decision variables for nonlinear optimization. The variable for thermal electricity generation is only active in the case where the stakeholder owns thermal generators and storage.

Variable	Symbol	Unit
Market price of electricity in hour i	p_i	€/kWh
Flow rate of water run through the turbines from reservoir k in hour i	$q_{i,k}^{dn}$	m^3/s
Flow rate of water pumped into reservoir k in hour i	$q_{i,k}^{up}$	m^3/s
"State of charge" of reservoir k in hour i	$S_{i,k}$	m^3
Electricity generated at thermal plant j in hour i	$w_{i,j}$	kWh

Table 4-5. Objective functions for each different type of owner

Eq	Owner	Formulation
4-1	Independent	$\max \sum_{i=1}^{n} \left(\sum_{k=1}^{5} \frac{-p_i g h_{i,k} q_{i,k}^{up}}{\eta_k^{up}} + \eta_k^{dn} p_i g h_{i,k} q_{i,k}^{dn} \right)$
4-2	Thermal fleet	$\max \sum_{i=1}^{n} \left[\left(\sum_{k=1}^{5} \frac{-p_i g h_{i,k} q_{i,k}^{up}}{\eta_k^{up}} + \eta_k^{dn} p_i g h_{i,k} q_{i,k}^{dn} \right) + \left(\sum_{j=1}^{J} (p_i - r_j) w_{i,j} \right) \right]$
4-3	Consumer	$\min \sum_{i=1}^{n} \left[p_i d_i + \sum_{k=1}^{5} \frac{p_i g h_{i,k} q_{i,k}^{up}}{\eta_k^{up}} - \eta_k^{dn} p_i g h_{i,k} q_{i,k}^{dn} \right]$

Table 4-6. Constraints for nonlinear optimization

Eq	Constraint	Formulation
4-4	Storage level in time t+1 must equal storage level in time t, plus or minus the charge or discharge of storage in time t	$S_{k,i+1} = S_{k,i} + q_{i,k}^{up} - q_{i,k}^{dn}$
4-5	Starting and ending condition of storage level	$S_{k,1} = S_{k,init}\ , S_{k,n} = S_{k,end}$
4-6	No changes to storage at horizon time step	$q_{n,k}^{up} = 0, q_{n,k}^{dn} = 0$
4-7	Bounds on thermal generation in the thermal + PHS ownership case	$0 \leq w_{i,j} \leq w_j^{max}$
4-8	Market price and volume relationship in hour i	$p_i = a_i \left(d_i + \sum_{k=1}^{5} q_{i,k}^{up} - q_{i,k}^{dn} \right) + b_i$
4-9	Storage charge and discharge must operate within pump and turbine design constraints	$0 \leq q_{i,k}^{up} \leq q_k^{up,max}, 0 \leq q_{i,k}^{dn} \leq q_k^{dn,max}$

4.2.3 Assumptions and Limitations

It is necessary to simulate the relationship between quantity of electricity and price to determine the effect of storage on market prices. While small scale electricity storage can be simulated as a linear optimization because it is a price taker, large scale electricity storage that can change market prices requires a nonlinear optimization. Sioshansi (2010) also used nonlinear optimization to simulate price-influencing storage capacity.[64] I use two linear best fit lines per day to approximate the relationship between traded volume and price in the Iberian electricity market. I split the day into two segments: 1 am to 9 am and 10 am to midnight. Spees (2008) used fitted curves to relate price to load in PJM.[71] I found that using two daily linear equations has a lower absolute mean y-error compared to using only one best fit line or using a quadratic curve. I chose this break because it had the lowest absolute mean y-error (2.04 €/hr) compared to all other hours of the day, using a single best fit line (2.56 €/hr), or using a curve (2.29 €/hr). Figure 4-1 shows a scatter plot of actual prices and two methods of determining best fit line. Figure 4-2 shows one week of observed prices compared to simulated prices using my method.

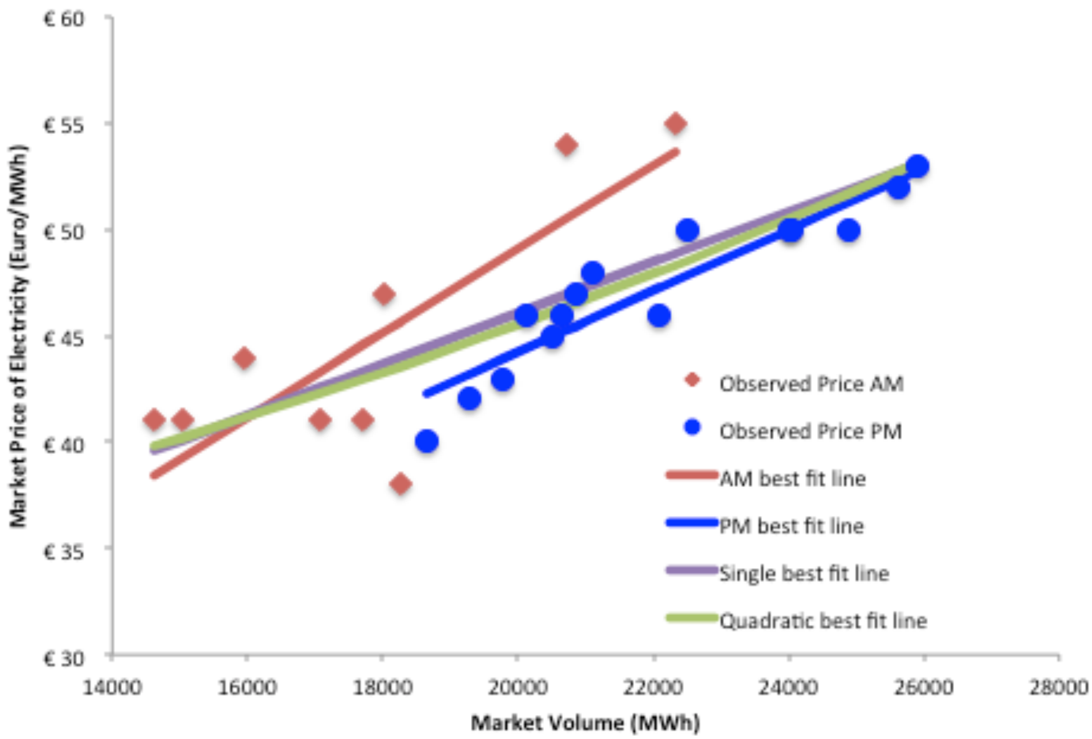

Figure 4-1. A scatter plot of one day of prices and market volumes (demand) with two best fit lines, one best fit line, and a quadratic. I use two best fit lines to characterize the price-demand relationship because this offers the lowest mean absolute error for predicting the price given a certain demand compared to using a single line or a higher order polynomial.

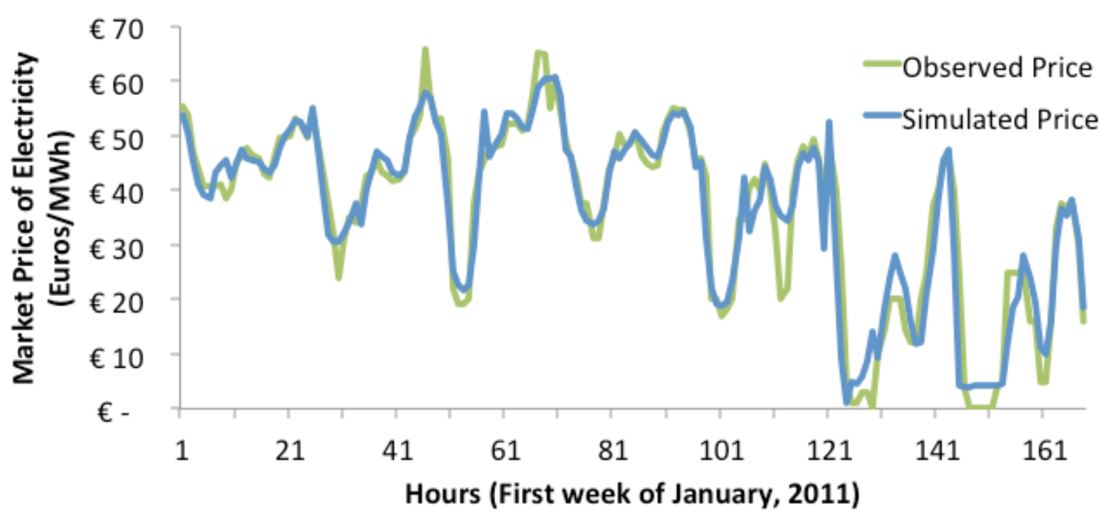

Figure 4-2. Observed and simulated prices in the MIBEL electricity market for January 1-7, 2011.

One limitation of simulating price data is that the best fit lines underestimate price spikes and troughs. If the storage operator had perfect knowledge of observed price extremes, he would be able to extract more value from arbitrage.

I simulate storage operations in two-week horizon optimization segments throughout the year. Simulating a complete two week period, rather than daily periods, is important because boundary conditions (at the start and end of a day) on dam volume restrict potential arbitrage profits significantly.

Throughout this paper, I also compare results using observed prices and simulated forecast prices to obtain bounds on potential benefits from storage. I simulate forecast data in two ways. First, I use the hourly average prices from 2008-2011. Second, I use prices from the previous week to make decisions about storage in the current week. I believe a trader would have access to better forecast information than my methods, and would therefore see results somewhere between my forecast and perfect information methods.

In my engineering model of the PHS facilities, I use a linear approximation of the relationship between head height and reservoir volume. This assumption is reasonable because the dams operate near full capacity where the change in volume due to generation and pumping has a very small effect on head height. An analysis of the relationship between head and volume for each dam is in Appendix 4B.

4.3 Results

4.3.1 Market Effects

Adding new storage capacity to the grid has the potential to reduce the variability of market prices in MIBEL. While a single PHS unit is effectively a price taker in MIBEL, the full 636 MW of new storage will significantly change market prices. Figure 4-3 compares simulated market prices in January 2011 to market prices in the case with 636 MW of new storage. Large storage penetration affects the arbitrage profit potential of individual storage owners and reduces price variability. For example, profits for the Gouvaes Iberdrola plant would be 21% lower when all new storage is added compared to the case when it operates alone. Sioshansi (2009) finds that 1 GW of storage in PJM would reduce the value of arbitrage profits of a price taker by 20%.[72] Figure 4-4 shows expected profits for each company when operating alone versus together. An individual storage plant is essentially a price taker, but when all 636 MW of storage capacity enters the market, market prices exhibit less variability.

Table 4-7 shows how prices will change statistically under the different ownership scenarios. While the mean daily price spread decreases under independent and consumer ownership, it increases under a thermal-storage ownership scenario. Figure 4-5 contains a price spread duration curve for each of the ownership scenarios. Both consumer and independent owners of storage reduce price spreads under optimal operations, but thermal storage owners increase them.

Table 4-7. Price statistics for all storage ownership cases and the no storage case. The set of prices used includes hourly data from four two-week periods (Winter, Spring, Summer and Fall). A full year of price effect data was not available for the PHS+Thermal case.

Euros/MWh	**No Storage**	**PHS**	**PHS+Consumer**	**PHS+Thermal**
Mean daily price spread	23.25	20.47	21.61	24.59
Mean price	47.47	47.77	46.87	48.31
Standard deviation	12.88	11.53	12.89	13.62

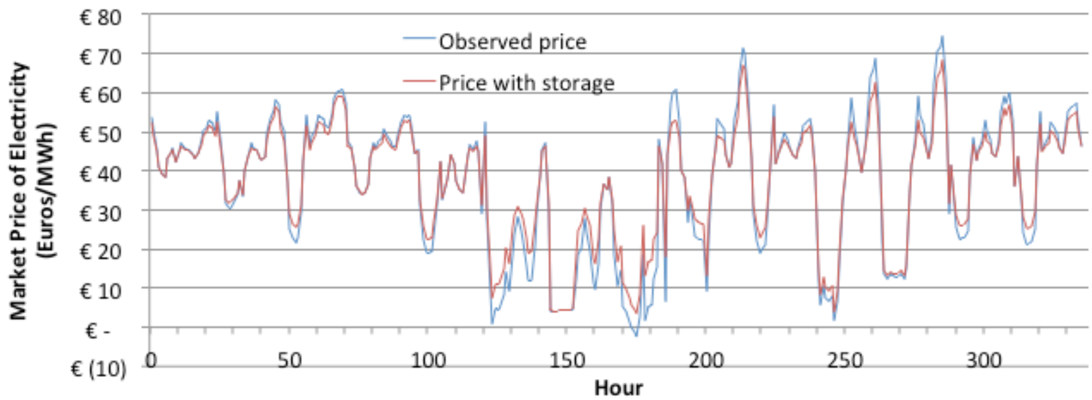

Figure 4-3. Simulated market prices and market prices with new storage added to the Portuguese electricity system. The time period is the first half of January 2011.

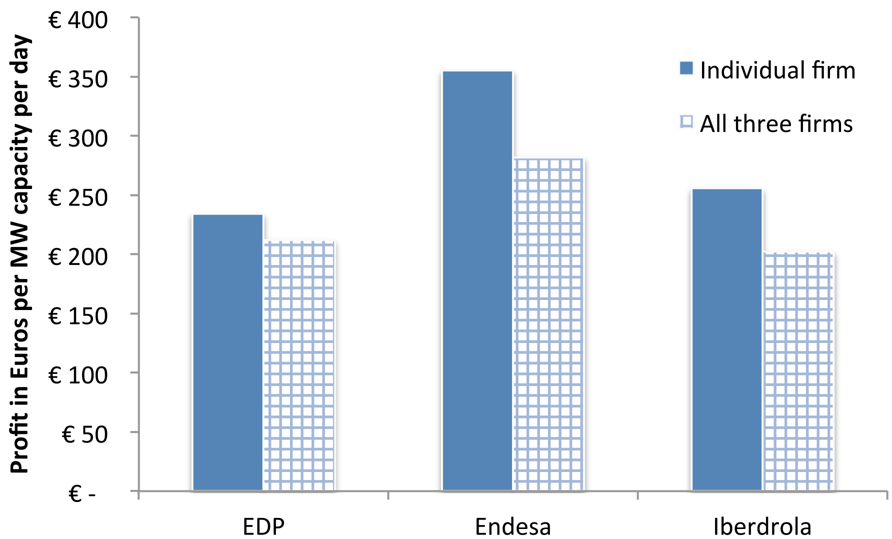

Figure 4-4. Bar chart showing the difference in expected profits for EDP, Iberdrola, and Endesa when operating alone versus operating together in the market. Endesa operates only the Girabolhos plant, which has a 77% round trip efficiency compared to 74-76% for the rest of the fleet.

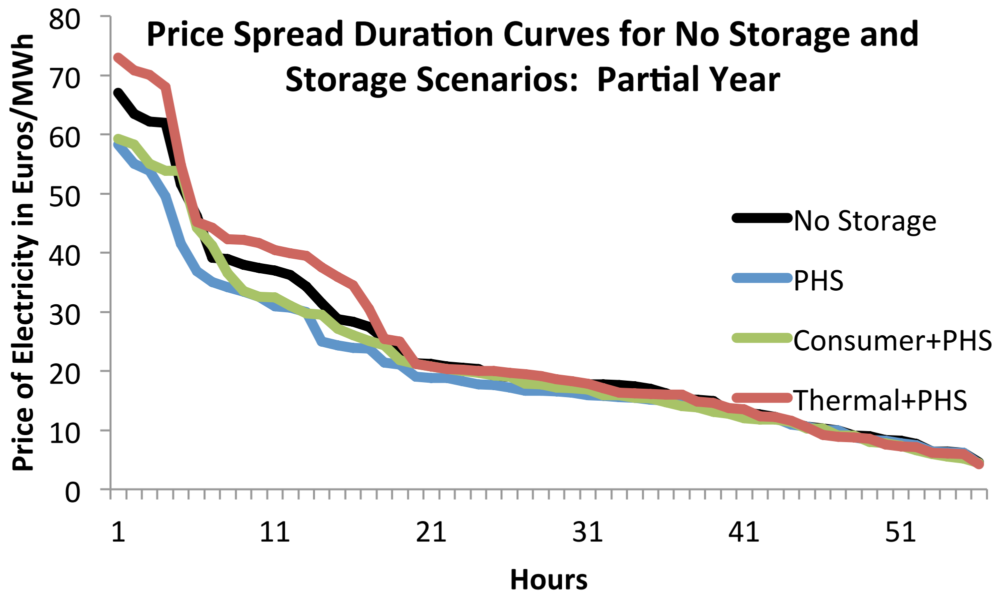

Figure 4-5. A price spread duration curve for the no storage, PHS, PHS+consumer, and PHS+thermal scenarios. Data was only available for four two-week periods during the year. PHS+thermal scenario creates bigger price spreads since this would help thermal plants increase profits. Lower price spreads (right side of graph) exhibit less variation between scenarios because storage is not used as much when the price spread is small in any of the storage ownership scenarios.

4.3.2 Independent Owner Arbitrage Profits

The goal of a company operating storage in MIBEL would be to maximize arbitrage profits, as long as it has no other competing interests in the same market. Using the nonlinear optimization model described in Section 4.2.2 I run the model for 26 two-week periods to simulate a year of operation. Using 2011 MIBEL Portugal price data, Figure 4-6 contains the arbitrage profit results for the five dam system. I note that arbitrage profit potential is much higher in the winter months compared to the rest of the year. Market prices exhibit greater spreads during the winter, allowing the storage units to extract greater value from arbitrage activities over a two week period. Figure 4-7 displays the market price spreads for 2008-2012 MIBEL price data for Portugal. All years follow a similar price trend, suggesting that results from 2011 would be indicative of results in other years.

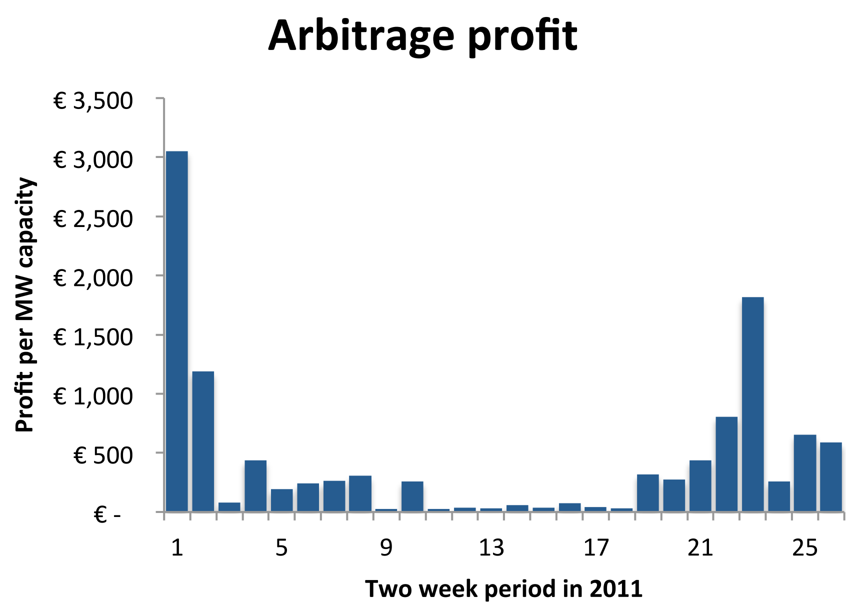

Figure 4-6. Arbitrage profit per MW capacity for the five dam system in the MIBEL electricity market in 2011. Profit is reported in two week intervals for the entire year.

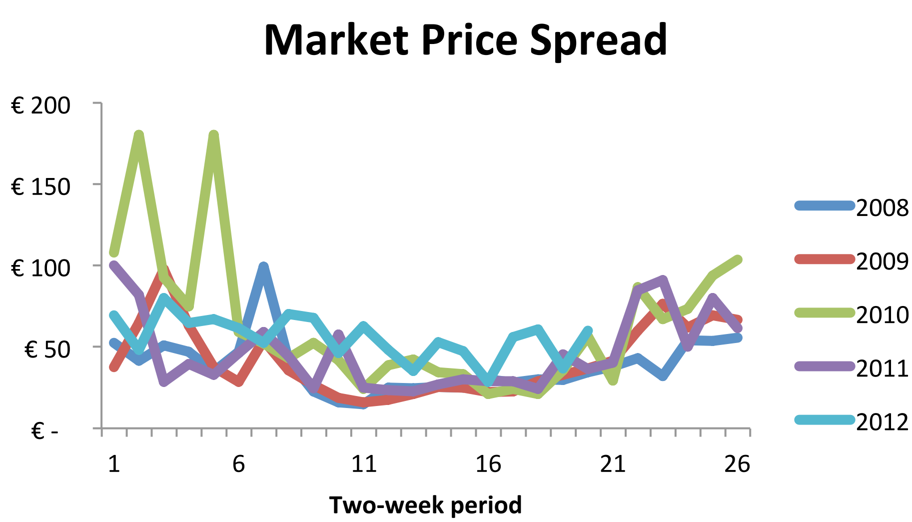

Figure 4-7. Two week maximum price spread for the MIBEL electricity market, 2008-2012.

The result that arbitrage profits are very low during all but the first and last months of the year is an interesting, if not discouraging finding, if one hopes to create a positive return on investment from storage in Portugal. Testing this model with data from another electricity market is instructive. The capacity of the Iberian market is similar to that of the California ISO (CAISO). If this exact system of PHS could operate in the California electricity market rather than MIBEL, much higher arbitrage profits would be expected. Figure 4-8 shows arbitrage profits for the PHS operating with CAISO data, and Figure 4-9 shows the maximum price spreads of CAISO in 2010 compared to those of MIBEL in Portugal.

I note that MIBEL in Portugal has a capacity market while CAISO does not. The capacity payments given to the PHS under MIBEL market rules could narrow the gap between expected profits from operation in MIBEL versus operation in CAISO.

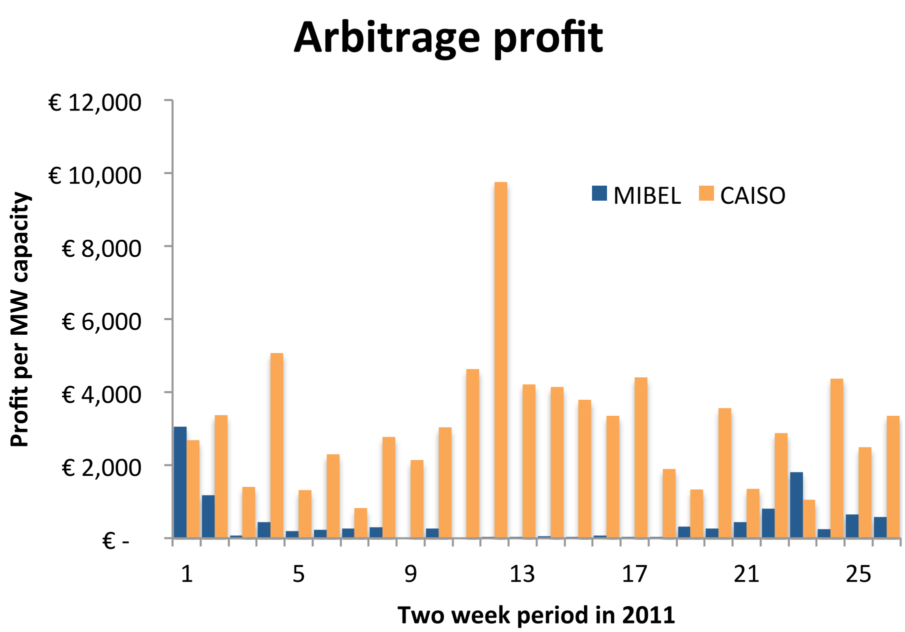

Figure 4-8. Arbitrage profit per MW capacity for the five dam system using prices from the CAISO electricity market in 2010. Profit is reported in two week intervals for the entire year. CAISO prices are converted to euros using a conversion of 1.3 USD = 1 Euro.

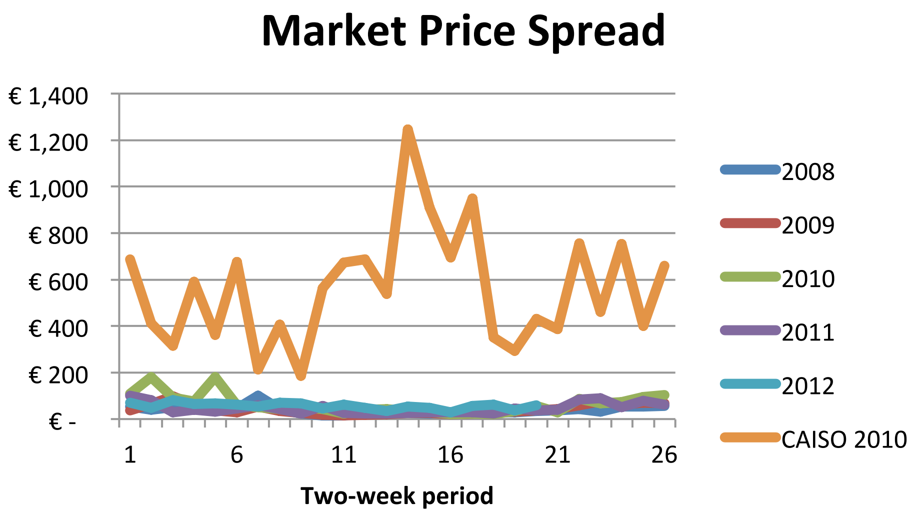

Figure 4-9. Two week maximum price spreads for the CAISO electricity market, 2010, compared to those in MIBEL, 2008-2012. CAISO prices are converted to euros using a conversion of 1.3 USD = 1 Euro.

4.3.2.1 Forecast Results

For actual storage operations, perfect knowledge of future market prices is not possible. Operators rely on forecasts or operation heuristics to inform electricity arbitrage. In order to provide a lower bound on profits, I show how profits from storage would change by using an average of observed market prices from 2008-2010 to optimize storage operations. Sioshansi (2009) used observed price data from the previous week to complete a week long optimization and found that 85-90% of potential profits could be realized.[72] Using MIBEL prices, I find that forecast results significantly reduce profits and in some cases eliminate profits all together (Figure 4-10). I found even lower expected arbitrage profits using a one-week backcast method.[h] Using CAISO market characteristics I find similarly poor results.

I also explore using a heuristic method that instructs an operator to buy energy during the low price period in the day and sell at the standard peak price period. Table 4-8 shows mean, median and mode hours for minimum and maximum daily price for MIBEL and

[h] The backcast method takes the average price for the previous seven days in each hour and uses that to estimate the expected price in the current hour.

CAISO markets, as well as expected arbitrage profits using heuristics compared to perfect information. Experimenting with different periods of buying and selling centered around either the mean, median, or mode minimum and maximum hours showed the best rule to follow was three hours each of buying and selling for MIBEL, and 7 hours each of buying and selling for CAISO. While these results are better than using a backcasting or annual average method, they still produce negative results in MIBEL and only 35% of the potential arbitrage profit for CAISO.

Table 4-8. Mean, median and mode of maximum and minimum price hours for the MIBEL and CAISO markets. Rightmost column shows the annual profit expected using only the heuristic rule applied to each hour. Third column shows annual profit from arbitrage using perfect information. All profits converted to Euros using the conversion 1.3 USD=1 Euro.

	Minimum hour	Maximum hour	Annual profit per MW: Perfect information	Annual profit per MW: heuristic
MIBEL 2011				
Mean	6.5	16.7	€11500	-€11200
Median	5	20		-€5226
Mode	5	22		-€4160
CAISO 2010				
Mean	5.9	16.1	€81600	€18800
Median	4	18		€28100
Mode	4	19		€28700

My results differ significantly from those of Siosanshi, who finds 80-90% of potential arbitrage value can be captured with a backcast. I believe the reason forecast arbitrage profits are low in CAISO is that past prices are relatively poor predictors of current prices, making it difficult to take advantage of large price spreads to create arbitrage profit. In the MIBEL market, the fact that the price spreads are so small most of the year means that only very precise storage operations could create an arbitrage profit. An analysis of PJM, MIBEL, and CAISO prices is shown in Appendix 4C. As someone operating in the MIBEL electricity market would have access to more sophisticated forecast methods than ours, the expected profits from arbitrage could be significantly higher than my forecast methods.

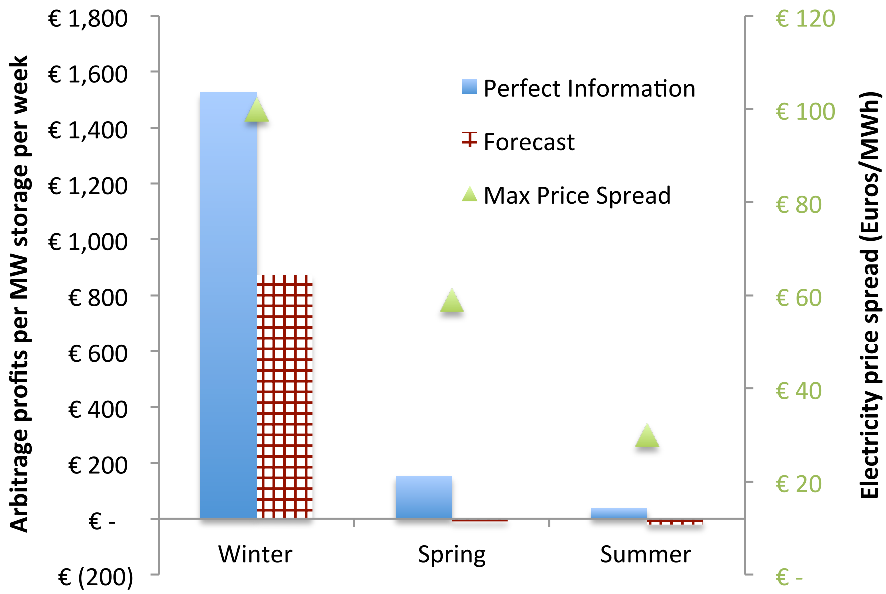

Figure 4-10. Storage arbitrage profits using observed prices versus using forecast prices for winter, spring, and summer cases. Arbitrage profit potential decreases as the maximum bi-weekly spread of market electricity prices decreases. The triangles represent the maximum electricity price spread in the corresponding two week simulation and correspond to the secondary y-axis.

4.3.3 Storage Ownership Effects

I examine three cases of storage ownership to illustrate how storage operations change depending on the incentives of the operator. In the previous section, an independent operator owns the PHS and operates them to maximize profits from energy arbitrage. In this section I show how storage operations change if the storage owner (1) also owns thermal generator assets that operate in the same market as the storage or (2) is the electricity consumer. These ownership structures create different outcomes regarding CO_2 emissions, thermal generator profits, and consumer expenditures on electricity.

Figure 4-11 illustrates how the different ownership scenarios create different decisions about how to operate the PHS.

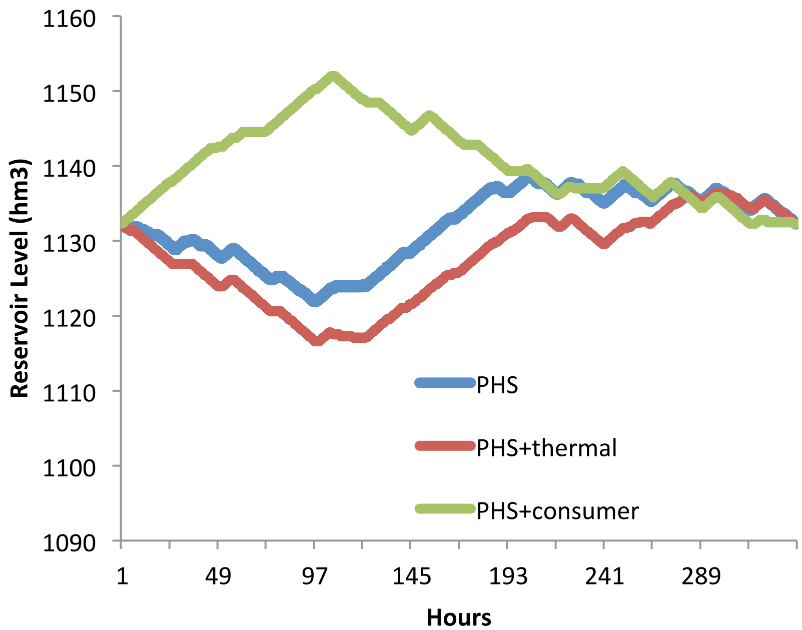

Figure 4-11. Storage levels of Foz Tua under independent operation, operation by an owner of thermal generation, and operation by a consumer entity during the Winter case. The different objectives lead to vastly different operation patterns.

4.3.3.1 Effects of Storage on Thermal Generators: CO_2 and Profits

I assume thermal generators operate when the market price of electricity exceeds their marginal cost of operation. This assumption disregards startup cost considerations, and is meant to be a first order approximation of how large-scale grid storage affects CO_2 emissions. I calculate changes in profit based on a combination of EDP's, Endesa's, and Iberdrola's thermal generator fleets in Portugal and Spain, which consists of 42% coal and 58% natural gas.

Figure 4-12 shows that thermal generator profits are highest under the scenario when storage is owned by a company that also owns thermal generation units. The profits under the thermal-owned case consist of arbitrage profits plus thermal generator profits. In the winter, most of the profit consists of arbitrage, which causes CO_2 emissions decrease as generators run less often. Under the independent owner case, CO_2 emissions generally increase as thermal generator profits decrease. CO_2 emissions increase under this scenario because higher minimum daily prices cause coal generators to run more often. At the same time, peak prices decrease and cut into thermal profit revenues. In the cases I examine, the reduction in peak hour profits is greater than the addition of profits in low price periods. My analysis accounts only for CO_2 emissions changes due to thermal generators, and not changes in emissions based on avoided wind curtailment.

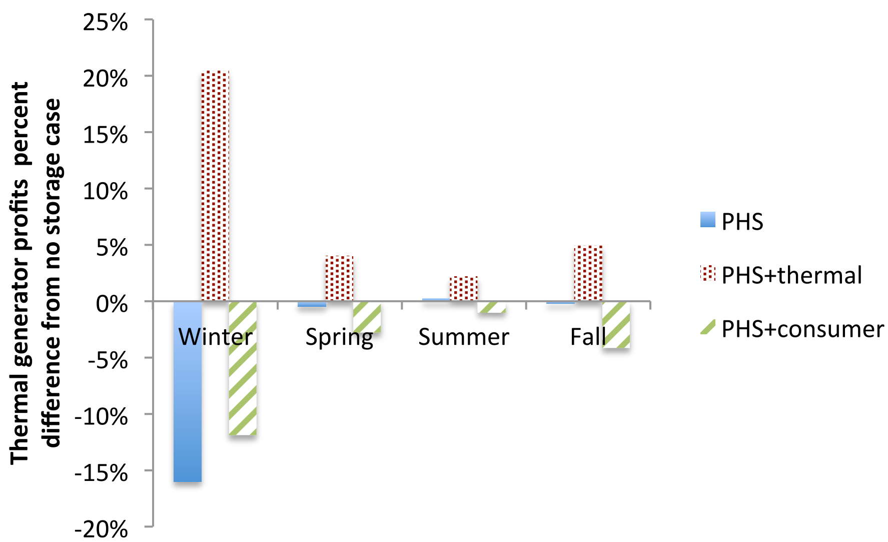

Figure 4-12. Percent change in thermal generator profits under different storage ownership conditions compared to the no storage case.

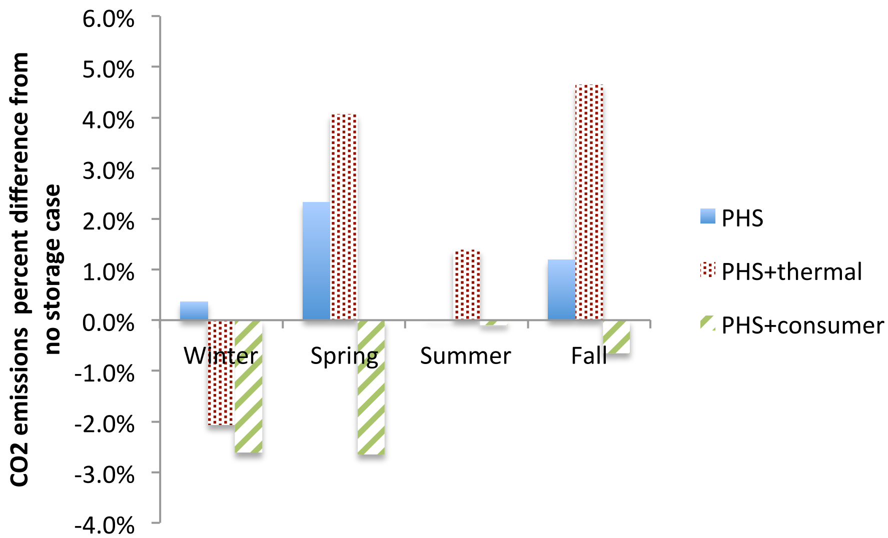

Figure 4-13. Percent change in CO_2 emissions from EDP thermal capacity in each season under different scenario conditions.

4.3.3.2 Effects of Storage on Consumers: Expenditure on Electricity

Changes to market prices will affect the total cost of providing electricity to consumers. I assume that the consumer expenditure on electricity related to energy traded in the MIBEL market for each hour is equal to the product of traded volume and price. Under independent and thermal ownership scenarios, the consumer expenditure on electricity increases (Figure 4-14). The only case where consumer expenditure on electricity decreases is when a consumer oriented entity owns the PHS. The contrast in the decision variable of reservoir level (Figure 4-11), contributes to the different results.

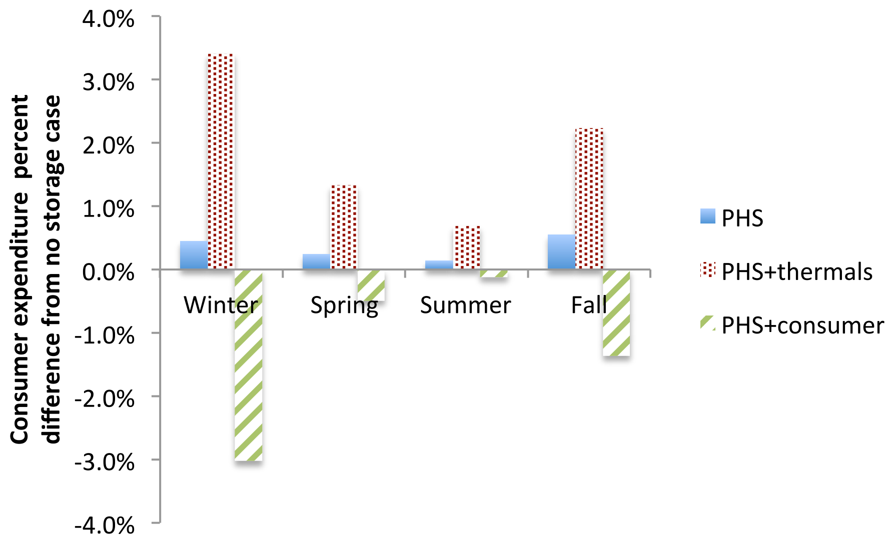

Figure 4-14. Change in consumer expenditures on electricity under different storage ownership conditions compared to the no storage case.

4.3.4 Financial Analysis of Storage Investment

Will private investment in electricity storage be cost effective? The five new PHS plants in Portugal are built into rivers and will also supply conventional hydropower. To calculate the cost effectiveness of the investment in the storage segment only, I must calculate the cost of PHS compared to traditional hydropower. The incremental costs of transforming a traditional hydro plant into a pumped hydro facility are hard to pin down. According to Energy Information Administration capital cost data, pumped hydro storage capital costs are about 80% higher than those of an equivalently sized traditional hydropower plant.[65]

I find that in the MIBEL market, arbitrage does not create a positive net present value for a private storage owner. However, when the storage owner is also an owner of thermal generation or is a consumer-oriented owner, then the investment would likely create a positive return using a 5% or 10% discount rate. My calculation of net present value does not include potential revenues from storage operating on the ancillary services market (which in Portugal is on the order of 300 MW), nor does it include revenues from conventional hydropower generation, which would pay for the capital costs of the dams not associated with storage. Hydro plants in Portugal also benefit from capacity payments, which help defray capital costs. For example, Alqueva I and II receive €4.8 million/yr or €9200/MW-yr for capacity availability.[73] I discuss other potential benefits and sources of revenue from storage in Section 4.4. In contrast, the net present value from arbitrage profits for an independent owner in the CAISO market would cover the capitol cost of the storage investment (Table 4-10).

Table 4-9. Capital costs of each pumped hydro plant per kW and costs attributable to storage. I use total costs from PNBEPH and EDP documents. Using EIA's estimate that pumping capabilities ad 80% to the cost of a hydro project, I estimate the segment of costs attributable to pumping.

Dam	**Capacity (MW)**	**Total cost (millions)**	**EIA estimate of storage segment (millions)**	**Storage cost (€ /kW)**
Girabolhos	72	€ 102	€ 46	€ 637
Gouvaes	112	€ 103	€ 47	€ 415
Alvito	48	€ 67	€ 30	€ 624
Foz Tua	234	€ 177	€ 80	€ 341
Baixo Sabor	170	€ 481	€ 217	€ 1,274
Total	636	€ 930	€419	€658 (weighted average)

Table 4-10. Net present value of storage with a 50-year outlook and independent ownership under MIBEL 2011 and CAISO 2010 conditions, and the capital cost of storage (all values are per kW capacity storage). All two week segments were calculated for PHS only and PHS+consumer, but due to long run times, the PHS+thermals calculations were extrapolated from the seasonal results.

<table>
<tr><th>Market</th><th>Ownership</th><th>5% Discount Rate</th><th>10% Discount Rate</th><th>Capital Cost</th></tr>
<tr><td rowspan="3">MIBEL 2011</td><td>PHS only</td><td>€210</td><td>€114</td><td rowspan="4">€658</td></tr>
<tr><td>PHS+thermals</td><td>€1410-2110</td><td>€765-1150</td></tr>
<tr><td>PHS+consumer</td><td>€1770</td><td>€960</td></tr>
<tr><td>CAISO 2010</td><td>PHS only</td><td>€1490</td><td>€808</td></tr>
</table>

Germany is considering adding 4.7 GW of new PHS to their 155 GW electric system.[74] This PHS capacity increase is similar to that of Portugal, both in terms of increase over current PHS capacity and in comparison to the total system capacity. Steffen assumes

80% efficiency and that the plants are price takers, and calculate that they would make €59,380/MW/year through electricity arbitrage. This is considerably higher than the Portuguese plant profit expectations through arbitrage: €11,500/MW/year for an independent storage owner. However, the price taker and 80% efficiency assumptions contribute to this discrepancy. Using technical specifications for the dams in Portugal, their roundtrip efficiencies range from 73-77%.

Previous literature also concludes that independent private investment in storage is not economically viable without a high carbon tax.[75, 76] My results show that while independent storage owners in MIBEL would not see a positive return on investment, thermal fleet owners and consumer-oriented owners likely would. Thermal owners see a positive return because they would be able to influence market prices with storage to run thermal plants longer and under higher prices. Consumer-oriented owners would be able to operate storage to decrease the total consumer expenditure on electricity. In reality, thermal fleet owners EDP, Endesa and Iberdrola have all invested in storage. Based on these results, the optimal operating strategy for thermal storage owners is to increase market price spreads to improve the profits of their thermal plants.

4.4 Conclusion and Policy Implications

I have shown that using PHS for arbitrage only will not create a positive return on investment in the MIBEL electricity market for an independent storage owner, but that a thermal fleet owner or consumer-oriented owner would benefit from the investment. Portugal wants to use storage to reduce wind curtailments, integrate distributed generation, and provide ancillary services to the grid. In 2010, wind provided 17% of total generation in Portugal.[58] Touhy and O'Malley (2009) find that storage is not a cost effective investment for reducing wind curtailment until wind provides over 50% of the total generation in the system.[77]

Another strong motivation behind using more hydropower is reducing Portugal's dependence on foreign imports of coal and natural gas. Portugal imports 100% of their coal and natural gas resources.[60] Most natural gas is purchased on long term take-or-pay contracts to ensure stable long term prices.[78]

If operated in a manner that reduces price spreads, new storage may eliminate the need for some of the most inefficient and rarely used capacity. However, my results show that a storage owner with thermal generation assets would operate storage to create the opposite effect.

I have shown that thermal fleet owners who also operate storage will do so in a way that does not meet Portugal's stated goals for investing in storage. To influence thermal storage owners to operate in a way that satisfies Portugal's requirements, Portugal must provide incentives to the storage operators that exceed the benefits of operating in a profit-maximizing way.

4.5 Appendix 4A: Technical Specifications of Dams

Dam	Owner	Volume (hm3)	Max head (m)	Min head (m)	Flow rate (m3/s)
Baixo Sabor	EDP	630	96	22	210
Foz Tua	EDP	649	127	77	220
Alvito	EDP	1155.42	86	6	65
Gouvães	Iberdrola	24.57	659	639	20
Girabolhos	Endesa	531	160	40	70

Dam	Optimal power (MW)	Efficiency (one way)	Efficiency (round trip)	Discharge time (days)	River
Baixo Sabor	170	0.86	0.74	34.7	Sabor
Foz Tua	234	0.86	0.73	16.3	Tua
Alvito	48	0.88	0.77	37.2	Ocreza
Gouvães	112	0.87	0.75	7.5	Torno
Girabolhos	72	0.88	0.77	23.6	Mondego

4.6 Appendix 4B: Volume-Head Relationship at Pumped Hydro Facilities

The flow of water into or out of the reservoir causes the volume of the reservoir to change, which affects the useful head of the water for power production. The following charts show the relationship between volume and head for each of the reservoirs (black diamonds), exponential fits (green) and linear fits (red). Because the reservoirs only operate at very near full conditions, the head-volume relationship can be simplified as linear, thus helping to eliminate nonlinear terms in the optimization constraints.

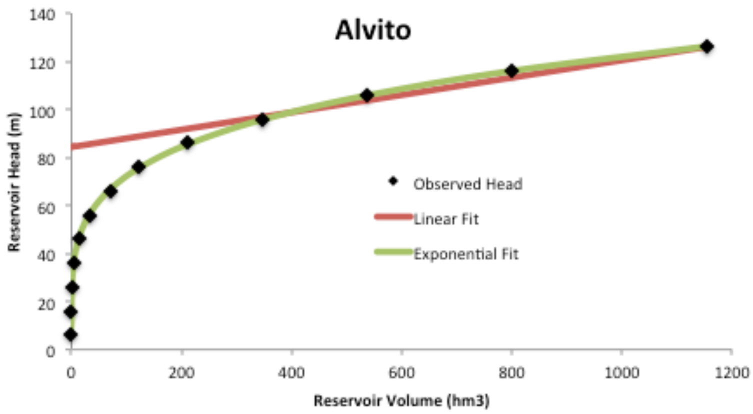

Figure 4-15. Head-volume relationship at Alvito pumped hydro facility.

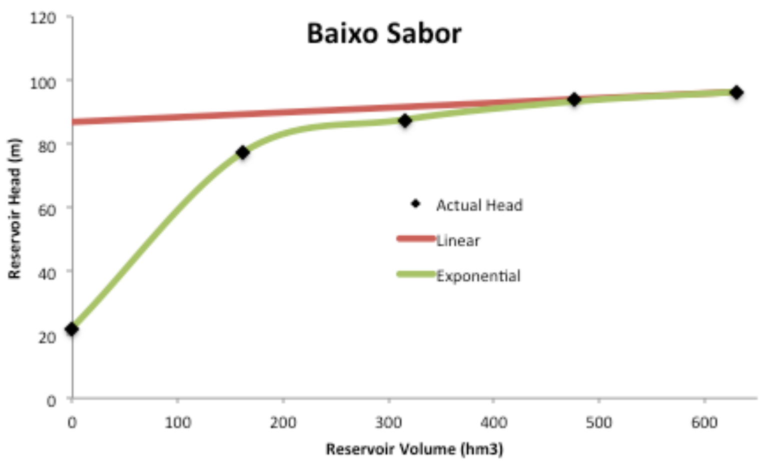

Figure 4-16. Head-volume relationship at Baixo Sabor pumped hydro facility.

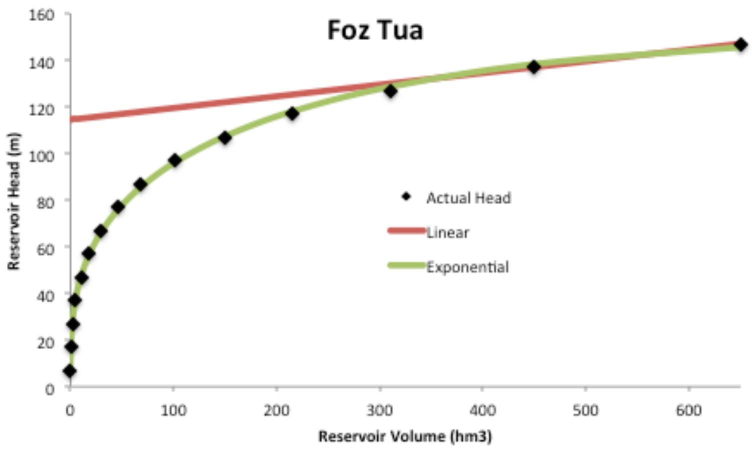

Figure 4-17. Head-volume relationship at Foz Tua pumped hydro facility.

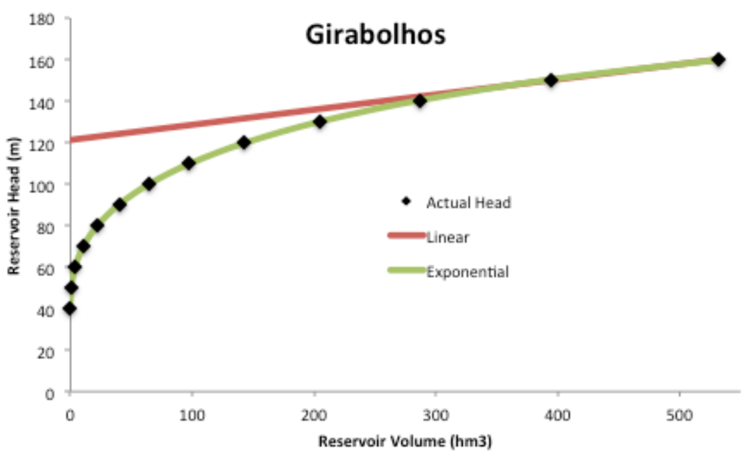

Figure 4-18. Head-volume relationship at Girabolhos pumped hydro facility.

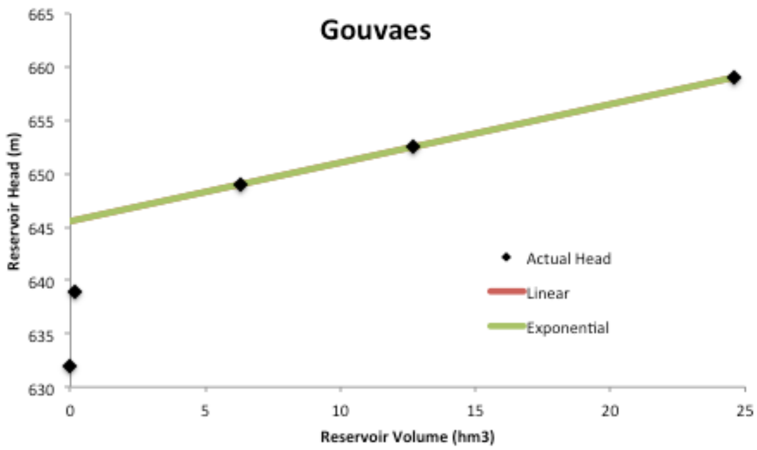

Figure 4-19. Head-volume relationship at Gouvaes pumped hydro facility. For this facility, the best fit exponential curve was linear.

4.7 Appendix 4C: Comparison of MIBEL, CAISO, and PJM market prices

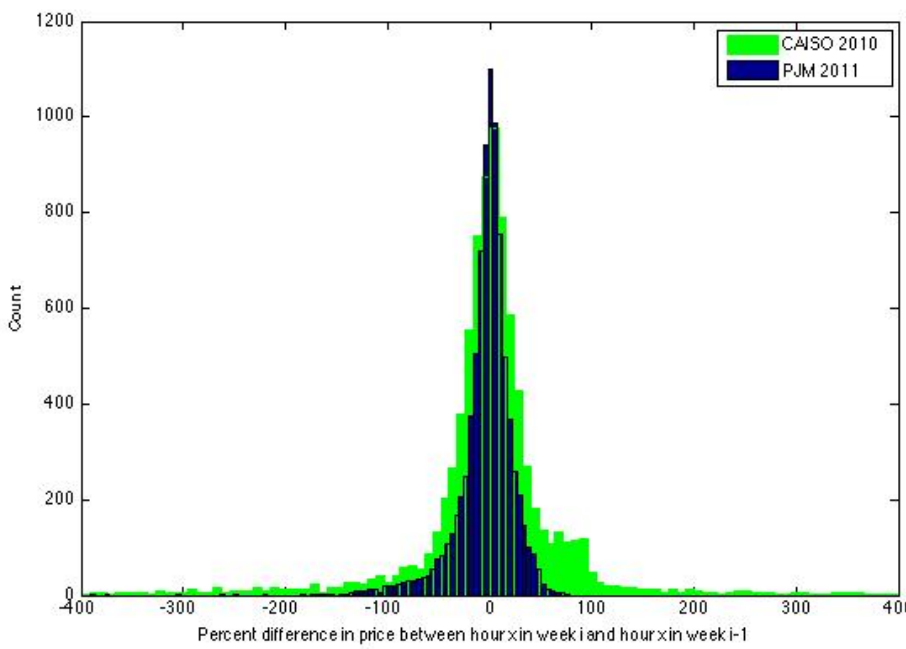

Figure 4-20. Histogram of the percent difference in hourly market price of electricity one week apart, comparing CAISO 2010 and PJM 2010 prices. The shape of the two graphs indicates that a one week backcast would better predict PJM prices than CAISO prices. This characteristic would contribute to better performance of storage arbitrage in the PJM market.

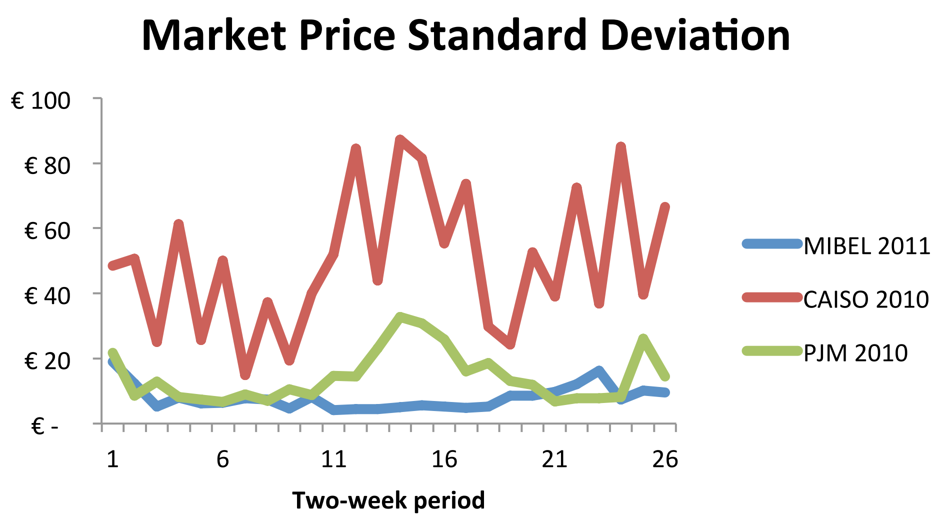

Figure 4-21. Standard deviation of prices in each two week period for CAISO, PJM, and MIBEL.

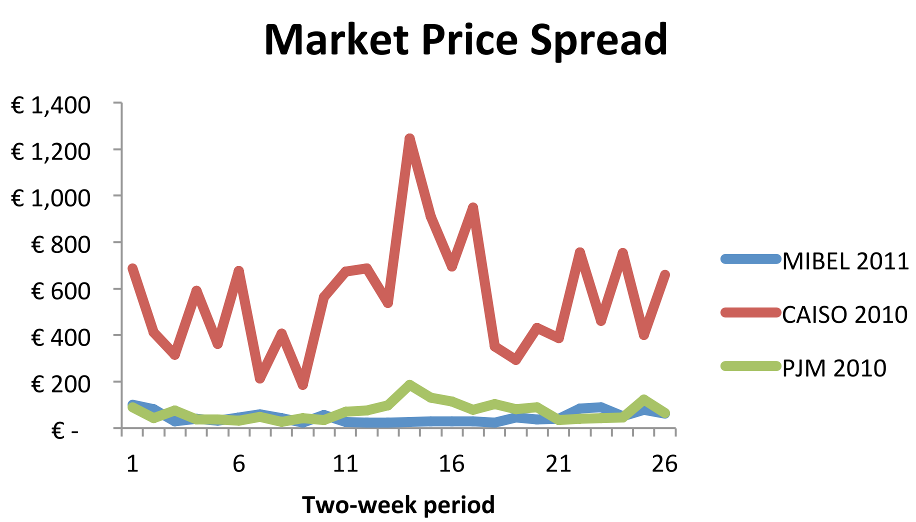

Figure 4-22. Maximum price spread during each two week period for CAISO, PJM, and MIBEL. Larger price spreads during the optimization periods allow for higher arbitrage profits. With low price spreads as in MIBEL, a storage owner cannot achieve significant profits without perfect knowledge of prices.

5. References

(1) Apt, J. The spectrum of power from wind turbines. *Journal of Power Sources* **2007**, *169*, 369–374.

(2) Katzenstein, W.; Fertig, E.; Apt, J. The variability of interconnected wind plants. *Energy Policy* **2010**, *38*, 4400–4410.

(3) Katzenstein, W.; Apt, J. *The Cost of Wind Power Variability*; CEIC-10-05; Carnegie Mellon Electricity Industry Center: Carnegie Mellon University, 2010.

(4) Lavania, C.; Rao, S.; Subrahmanian, E. Reducing Variation in Solar Energy Supply Through Frequency Domain Analysis. *IEEE Systems Journal* **2011**.

(5) Gowrisankaran, G.; Reynolds, S.; Samano, M. *Intermittency and the Value of Renewable Energy*; University of Arizona.

(6) Mills, A.; Wiser, R. *Implications of Wide-Area Geographic Diversity for Short-Term Variability of Solar Power.*; LBNL-3884E; Lawrence Berkeley National Laboratory, 2010; p. 49.

(7) Dobesova, K.; Apt, J.; Lave, L. B. Are Renewables Portfolio Standards Cost-Effective Emission Abatement Policy? *Environmental Science & Technology* **2005**, *39*, 8578–8583.

(8) Clean Air Markets - Data and Maps. http://camddataandmaps.epa.gov/gdm/index.cfm?fuseaction=iss.progressresults (accessed October 25, 2011).

(9) FERC *Integration of Variable Energy Resources 18 CFR Part 35*; 133 FERC 61149; Federal Energy Regulatory Commission, 2010; p. 122.

(10) Katzenstein, W.; Apt, J. Air Emissions Due To Wind And Solar Power. *Environ. Sci. Technol.* **2009**, *43*, 253–258.

(11) NREL Solar Prospector Map. http://maps.nrel.gov/prospector (accessed August 6, 2011).

(12) Acciona North America Energy Basics: Semiconductors and the Built-In Electric Field for Crystalline Silicon Photovoltaic Cells. http://www.eere.energy.gov/basics/renewable_energy/semiconductors.html (accessed August 5, 2011).

(13) Gnadt, P. *Automating electric utility distribution systems : the Athens Automation and Control Experiment*; Prentice Hall: Englewood Cliffs N.J., 1990.

(14) Baran, M.; Wu, F. Network Reconfiguration in Distribution Systems for Loss Reduction and Load Balancing. *IEEE Transactions on Power Delivery* **1989**, *4*, 1401–1408.

(15) Glamocanin, V. Optimal loss reduction of distributed networks. *IEEE Trans. Power Syst.* **1990**, *5*, 774–782.

(16) Shirmohammadi, D.; Hong, H. W. Reconfiguration of electric distribution networks for resistive line losses reduction. *IEEE Trans. Power Delivery* **1989**, *4*, 1492–1498.

(17) Taleski, R.; Rajicic, D. Distribution network reconfiguration for energy loss reduction. *IEEE Trans. Power Syst.* **1997**, *12*, 398–406.

(18) Kashem, M. A.; Ganapathy, V.; Jasmon, G. B. Network reconfiguration for enhancement of voltage stability in distribution networks. *IEE Proc., Gener. Transm. Distrib.* **2000**, *147*, 171.

(19) Shirmohammadi, D. Service restoration in distribution networks via network reconfiguration. *IEEE Trans. Power Delivery* **1992**, *7*, 952–958.
(20) Carvalho, P. M. S.; Correia, P. F.; Ferreira, L. A. F. M. Mitigation of Interruption Reimbursements by Periodic Network Reconfiguration: Risk-Based Versus Expected-Value Optimization. *IEEE Trans. Power Syst.* **2007**, *22*, 845–850.
(21) Nabaei, V.; Zareiegovar, G.; Mohammadi, M.; Jannesar, A. Distribution Network Reliability Enhancement for Minimizing Penalty Cost. In; IEEE: Prague, CZ, 2010; pp. 354–357.
(22) Choi, J. H.; Kim, J. C.; Moon, S. I. Integration operation of dispersed generations to automated distribution networks for network reconfiguration. In *2003 IEEE Bologna Power Tech Conference Proceedings,*; Bologna, Italy, 2003; pp. 408–412.
(23) Celli, G.; Loddo, M.; Pilo, F.; Abur, A. On-line network reconfiguration for loss reduction in distribution networks with Distributed Generation. In *CIRED, 2005*; Turin, Italy, 2005.
(24) Subrahmanyam, J. B. V.; Radhakrishna, C. Impact of DGs on Reconfiguration of Unbalanced Radial Distribution Systems. *Acta Electrotehnica* **2010**, *51*, 92–98.
(25) Subrahmanyam, J. B. V.; Radhakrishna, C. Impact of Wind Energy Modeled Distributed Generation on Reconfiguration of Unbalanced Radial Distribution System. *Research Journal of Applied Sciences, Engineering and Technology* **2010**, *2*, 252–261.
(26) Broadwater, R.; Khan, A.; Shaalan, H.; Lee, R. Time Varying Load Analysis To Reduce Distribution Losses Through Reconfiguration. *IEEE Transactions on Power Delivery* **1993**, *8*, 294–300.
(27) Lopez, E.; Opazo, H.; Garcia, L.; Bastard, P. Online Reconfiguration Considering Variability Demand: Applications to Real Networks. *IEEE Trans. Power Syst.* **2004**, *19*, 549–553.
(28) Zhou, Q.; Shirmohammadi, D.; Liu, W. H. E. Distribution feeder reconfiguration for operation cost reduction. *IEEE Trans. Power Syst.* **1997**, *12*, 730–735.
(29) ERCOT - Hourly Load Data Archives. http://www.ercot.com/gridinfo/load/load_hist/ (accessed March 31, 2011).
(30) Carvalho, P. M. S.; Ferriera, L. A. F. M.; Barruncho, L. F. M. On Spanning-Tree Recombination in Evolutionary Large-Scale Network Problems - Application to Electrical Distribution Planning. *IEEE Transactions on Evolutionary Computation* **2001**, *5*, 623–630.
(31) Chiou, J. P.; Chang, C. F.; Su, C. T. Variable Scaling Hybrid Differential Evolution for Solving Network Reconfiguration of Distribution Systems. *IEEE Trans. Power Syst.* **2005**, *20*, 668–674.
(32) Nara, K.; Shiose, A.; Kitagawa, M.; Ishihara, T. Implementation of genetic algorithm for distribution systems loss minimum re-configuration. *IEEE Trans. Power Syst.* **1992**, *7*, 1044–1051.
(33) Mendoza, J.; Lopez, R.; Morales, D.; Lopez, E.; Dessante, P.; Moraga, R. Minimal Loss Reconfiguration Using Genetic Algorithms With Restricted Population and Addressed Operators: Real Application. *IEEE Trans. Power Syst.* **2006**, *21*, 948–954.

(34) de Queiroz, L. M. O.; Lyra, C. A Genetic Approach for Loss Reduction in Power Distribution Systems under Variable Demands. In *2006 IEEE International Conference on Evolutionary Computation*; Vancouver, BC, Canada, 2006; pp. 2691–2698.
(35) Olamaei, J.; Niknam, T.; Gharehpetian, G. Application of particle swarm optimization for distribution feeder reconfiguration considering distributed generators. *Applied Mathematics and Computation* **2008**, *201*, 575–586.
(36) Olamaei, J.; Gharehpetian, G.; Niknam, T. An approach based on Particle Swarm Optimization for distribution feeder reconfiguration considering Distributed Generators. In *2007 Power Systems Conference: Advanced Metering, Protection, Control, Communication, and Distributed Resources*; Clemson, SC, USA, 2007; pp. 326–330.
(37) Chiang, H. D.; Jean-Jumeau, R. Optimal network reconfigurations in distribution systems. I. A new formulation and a solution methodology. *IEEE Trans. Power Delivery* **1990**, *5*, 1902–1909.
(38) Jeon, Y. J.; Kim, J. C.; Kim, J. O.; Lee, K. Y.; Shin, J. R. An Efficient Simulated Annealing Algorithm for Network Reconfiguration in Large-Scale Distribution Systems. *IEEE Power Eng. Rev.* **2002**, *22*, 61–62.
(39) Carvalho, P. M. S.; Ferreira, L. A. F. M.; Cerejo da Silva, A. J. A Decomposition Approach to Optimal Remote Controlled Switch Allocation in Distribution Systems. *IEEE Trans. Power Delivery* **2005**, *20*, 1031–1036.
(40) ERCOT - Balancing Energy Services Market Clearing Prices for Energy. http://www.ercot.com/mktinfo/prices/mcpe (accessed December 16, 2010).
(41) Shirmohammadi, D.; Hong, H. W.; Semlyen, A.; Luo, G. X. A compensation-based power flow method for weakly meshed distribution and transmission networks. *IEEE Trans. Power Syst.* **1988**, *3*, 753–762.
(42) Zimmerman, R. D.; Hsiao-Dong Chiang Fast decoupled power flow for unbalanced radial distribution systems. *IEEE Trans. Power Syst.* **1995**, *10*, 2045–2052.
(43) Rajicic, D.; Dimitrovski, A. A New Method for Handling PV Nodes in Backward/Forward Power Flor for Radial and Weakly Meshed Networks. In; IEEE: Porto, Portugal, 2001.
(44) Afsari, M.; Singh, S. P.; Raju, G. S.; Rao, G. K. A Fast Power Flow Solution of Radial Distribution Networks. *Electric Power Components and Systems* **2002**, *30*, 1065–1074.
(45) Liu, W.; Ning, W. H.; Huang, D. S. A Modified Power Flow Calculation Method for Radial Distribution System. In; IEEE, 2008.
(46) Augugliaro, A.; Dusonchet, L.; Favuzza, S.; Ippolito, M. G.; Sanseverino, E. R. A backward sweep method for power flow solution in distribution networks. *International Journal of Electrical Power & Energy Systems* **2010**, *32*, 271–280.
(47) Vinoth Kumar, K.; Selvan, M. P. A simplified approach for load flow analysis of radial distribution network with embedded generation. In; IEEE, 2008; pp. 1–6.
(48) BPA: Balancing Authority Load & Total Wind Generation. http://www.transmission.bpa.gov/business/operations/wind/ (accessed September 8, 2010).

(49) Fisher, E. B.; O'Neill, R. P.; Ferris, M. C. Optimal Transmission Switching. *IEEE Trans. Power Syst.* **2008**, *23*, 1346–1355.
(50) Stoupis, J. **2010**.
(51) Carvalho, P. Line Costs **2011**.
(52) Energy Information Administration Table 8.1 Electricity Overview, 1949-2009 (Billion Kilowatthours). http://www.eia.doe.gov/emeu/aer/txt/ptb0801.html (accessed December 14, 2010).
(53) BPA - Energy Smart Utility Efficiency. http://www.bpa.gov/energy/n/industrial/Distribution/ (accessed December 14, 2010).
(54) MIBEL OMIP. http://www.omip.pt/Downloads/tabid/104/language/en-GB/Default.aspx (accessed October 20, 2012).
(55) Paish, O. Small hydro power: technology and current status. *Renewable and Sustainable Energy Reviews* **2002**, *6*, 537–556.
(56) EDP Special Regime. http://www.edp.pt/en/aedp/unidadesdenegocio/producaodeelectricidade/Pages/RegimeEspecial.aspx (accessed November 16, 2012).
(57) European Union The EU climate and energy package - Policies - Climate Action - European Commission. http://ec.europa.eu/clima/policies/package/index_en.htm (accessed October 20, 2012).
(58) Silva, R. Merits of hydroelectric pumped-storage schemes in the management of intermittent natural energy resources in Portugal **2011**.
(59) EDP Complementaridade Hídrica-Eólica - Centros Produtores | edp - viva a nossa energia. http://www.a-nossa-energia.edp.pt/centros_produtores/complementariedade_hidroeolica_he.php (accessed December 15, 2012).
(60) Energy Information Administration Independent Statistics & Analysis: Portugal. http://www.eia.gov/countries/country-data.cfm?fips=PO (accessed October 20, 2012).
(61) Endesa Spain and Portugal Endesa.com. http://www.endesa.com/en/aboutEndesa/businessLines/Electricity/SpainAndPortugal (accessed November 16, 2012).
(62) Iberdrola *Resultados: Informe Trimestral*; 2011.
(63) EDP Produção de Electricidade. http://www.edp.pt/pt/aedp/unidadesdenegocio/producaodeelectricidade/Pages/ProducaoElectricidade.aspx (accessed November 16, 2012).
(64) Sioshansi, R. Welfare Impacts of Electricity Storage and the Implications of Ownership Structure. *The Energy Journal* **2010**, *31*.
(65) Energy Information Administration *Updated Capital Cost Estimates for Electricity Generation Plants*; Department of Energy: Washington, DC, 2010.
(66) MIBEL Market Price and Traded Volume Data. http://www.omip.pt/Downloads/DerivadosdeElectricidade/tabid/104/language/en-US/Default.aspx (accessed October 15, 2012).
(67) PNBEPH PNBEPH /Home. http://pnbeph.inag.pt/np4/home.html (accessed October 15, 2012).

(68) EDP Novas Barragens - Centros Produtores | edp - viva a nossa energia. http://www.a-nossa-energia.edp.pt/centros_produtores/empreendimento_type.php?e_type=nb (accessed October 15, 2012).
(69) CAISO Market Price and Load Data. http://oasis.caiso.com.
(70) Tomlab Optimization *Tomlab*; Tomlab Optimiztion, 2012.
(71) Spees, K. Meeting Electric Peak on the Demand Side: Wholesale and Retail Market Impacts of Real-Time Pricing and Peak Load Management Policy, Carnegie Mellon University: Pittsburgh, PA, 2008.
(72) Sioshansi, R.; Denholm, P.; Jenkin, T.; Weiss, J. Estimating the value of electricity storage in PJM: Arbitrage and some welfare effects. *Energy Economics* **2009**, *31*, 269–277.
(73) Subsídos que a factura eléctrica paga. *Público* **2012**.
(74) Steffen, B. Prospects for pumped-hydro storage in Germany. *Energy Policy* **2012**, *45*, 420–429.
(75) Fertig, E.; Apt, J. Economics of compressed air energy storage to integrate wind power: A case study in ERCOT. *Energy Policy* **2011**, *39*, 2330–2342.
(76) Mauch, B.; Carvalho, P. M. S.; Apt, J. Can a wind farm with CAES survive in the day-ahead market? *Energy Policy* **2012**, *48*, 584–593.
(77) Tuohy, A.; O'Malley, M. Impact of pumped storage on power systems with increasing wind penetration. In; IEEE, 2009; pp. 1–8.
(78) Melling, A. *Natural Gas Pricing and Its Future: Europe as the Battleground*; Carnegie Endowment for International Peace: Washington, DC, 2010.